NACA

RESEARCH MEMORANDUM

WIND-TUNNEL INVESTIGATION OF A 1/6-SCALE MODEL OF THE BUMBLEBEE XPM MISSILE AT HIGH SUBSONIC SPEEDS

By Warren H. Nelson

Ames Aeronautical Laboratory
Moffett Field, Calif.

NATIONAL ADVISORY COMMITTEE FOR AERONAUTICS

WASHINGTON
December 11, 1950

NATIONAL ADVISORY COMMITTEE FOR AERONAUTICS

RESEARCH MEMORANDUM

WIND-TUNNEL INVESTIGATION OF A 1/6-SCALE MODEL OF THE BUMBLEBEE XPM MISSILE AT HIGH SUBSONIC SPEEDS

By Warren H. Nelson

SUMMARY

The results of an investigation of a 1/6-scale model of the Bumblebee XPM missile to determine the causes of booster-fin failures on the full-scale missile are presented. The Mach number range was 0.20 to 0.94, and the corresponding Reynolds number range was 525,000 to 1,555,000, based on the body diameter. It was concluded that the failures of the fins were due to launching shoes which caused the missile to trim at increasingly negative angles of attack as the Mach number increased up to 0.86. Under these conditions, the booster fins apparently became overloaded to the point of failure.

Additional tests were made with wing spoilers and alternate booster fins to determine their effect on stability. The wing spoilers were effective in increasing the stability except at low Mach numbers and small angles of attack. The alternate booster fins increased the stability by an amount equal to a neutral-point shift of 6 percent of the total missile length.

INTRODUCTION

The launching of the first full-scale Bumblebee LT V-3 (XPM) test vehicle from a ramp was successful and normal accelerated flight occurred for about 2 seconds. At this point, all four booster fins were torn loose from the booster body in less than one-thirtieth of a second. From the analysis of flight data it was thought that the failure occurred at a Mach number close to 1.0, and that the angle of attack increased markedly prior to failure. Careful study of the data and the recovered components indicated that possible causes could be: (1) a large decrease in longitudinal stability just before failure, and (2) progressive twisting of the booster fins due to torsional weakness. As a result, a second test vehicle on which the torsional rigidity of the fins was greatly increased was launched. The results were identical with those for the first vehicle. The large torsional rigidity which was built into the fins ruled out fin torsional weakness as the primary cause of failure. Consequently, the basic cause was thought to be the decrease in longitudinal stability.

In order to investigate the reason and possible remedies for the booster-fin failures, and to obtain data at a reasonably large Reynolds number and at speeds close to sonic, tests of a 1/6-scale model of the Bumblebee XPM missile were conducted in the Ames 16-foot high-speed wind tunnel. These tests were made at the request of the Bureau of Ordnance, Department of the Navy.

Additional tests were made of the model with wing incidence varied, with wing spoilers, with alternate booster fins, and in various rolled positions to determine the effect of these variables on stability.

NOTATION

The coefficients used in this report differ from the standard nomenclature in that the body-cross-section area is used instead of the wing area, the missile length is used in place of the wing mean aerodynamic chord, and the body diameter is used in calculating Reynolds number.

C_m pitching-moment coefficient about the center of gravity $\left(\frac{\text{moment}}{qSl}\right)$ (Center of gravity at 0.598 l with short booster, 0.565 l with long booster)

C_N normal-force coefficient $\left(\frac{N}{qS}\right)$

M Mach number

N normal force, pounds

P pressure coefficient $\left(\frac{p-p_o}{q}\right)$

P_{cr} critical pressure coefficient

R Reynolds number $\left(\frac{Vd}{\nu}\right)$

S area of body cross section, square feet

V free-stream velocity, feet per second

d body diameter, feet

l body length (including booster), feet (Body length with short booster, 4.97 ft; with long booster, 5.41 ft)

p local static pressure, pounds per square foot

p_o free-stream static pressure, pounds per square foot

q dynamic pressure $\left(\frac{1}{2}\rho V^2\right)$, pounds per square foot

α angle of attack of body center line, degrees

α_t angle of attack for trim, degrees

ν kinematic viscosity, square feet per second

ρ density, slugs per cubic foot

MODEL AND APPARATUS

A 1/6-scale model of the Bumblebee XPM missile was supplied by the Applied Physics Laboratory of The Johns Hopkins University for these tests. The basic dimensions of the model are given in figure 1. Figure 2 is a photograph of the model mounted in the Ames 16-foot high-speed wind tunnel.

Forces on the model were measured by means of strain gages mounted on the sting. With the strain gages mounted as they were, it was possible to ascertain only normal force and pitching moment. The angle of attack of the model was measured by optical means.

Two booster lengths were provided: modification II (short booster) and modification III (long booster). The contractor's nomenclature for the booster lengths has been used here; however, in the remainder of this report, modifications II and III will be referred to as the short and long boosters, respectively. The short booster was provided so that the configuration that failed in flight could be tested; however, the long booster has since superseded the short one.

TESTS

The investigation was conducted at Mach numbers from 0.20 to 0.94 and corresponding Reynolds numbers from 525,000 to 1,550,000 (based on body diameter), as shown in figure 3. The maximum Mach numbers obtained were limited by the power available to the wind tunnel.

Tests were made of the original model with various launching-shoe positions, including symmetrically mounted shoes. The optimum shoe positions were then used on the revised model during tests of wing spoilers, of various wing incidences, of alternate booster fins with the missile-booster combination in rolled attitudes, and of the missile rolled relative to the booster. The short booster, hoisting lugs, and launching shoes of the original model were replaced by a long booster, modified hoisting lugs, and launching shoes on the revised model.

Constriction corrections were applied to the tunnel-empty calibration according to the methods of reference 1. Tunnel-wall corrections were not applied since they were within the accuracy of the data.

RESULTS AND DISCUSSION

This section is in two parts: The first covers a discussion of the results of tests to determine the causes of the fin failures on the original missile, and methods developed to alleviate these failures; and the second part covers a discussion of the results of tests of the revised model.

Aerodynamic Characteristics of the Original Model

The first model tested in the Ames 16-foot high-speed wind tunnel represented the Bumblebee RTV-N-6a (XPM) missile. The results indicated that at 0° angle of attack there existed a positive lift (except for Mach numbers below 0.70) and a negative pitching moment (figs. 4 and 5). The trim angles indicated by extrapolation of the pitching-moment curves decreased from -0.9° at 0.2 Mach number to -6.7° at 0.88 Mach number, then increased to -4.9° at 0.94 Mach number as shown in figure 6. With the exception of the hoisting lugs and launching shoes (fig. 7), the model was symmetrical. To check the effects of air-stream angle, the model was tested in an inverted position. The results (figs. 4 and 5) show a positive pitching moment equal in magnitude to the negative pitching moment experienced in the normal position, thus confirming the asymmetry of the model characteristics.

Since the hoisting lugs and launching shoes were the only unsymmetrical parts of the original model, they were removed and tests were made. The data shown in figures 4 and 5 indicate essentially zero moment at 0° angle of attack for this condition; the small negative pitching moment and normal force that did exist can be attributed to slight misalinements of the model. The trim-angle change with Mach number for the original model less hoisting lugs and launching shoes, as shown in figure 6, is at most -0.6°. The previously mentioned trim angles are based on the location of the center-of-gravity position at zero Mach number. The center of gravity of the full-scale vehicle moves forward linearly as the Mach number increases, the distance moved in inches being equal to 12.5 times the Mach number. Applying this relationship to the wind-tunnel data increases the trim angle as shown in figure 6.

The normal-force and stability parameters $dC_N/d\alpha$ and dC_m/dC_N are presented as a function of Mach number in figure 8, and are the average slopes near zero normal force. In general, there was a slight decrease in stability as the Mach number was increased. The normal-force parameter $dC_N/d\alpha$ remained essentially constant up to a Mach number of 0.70, then increased. Removing the hoisting lugs and the launching shoes had little effect on the normal-force and stability parameters $dC_N/d\alpha$ and dC_m/C_N.

The relative values of the positive lift and the negative pitching moment existing at 0° angle of attack with the hoisting lugs and the launching shoes in position indicated that the pitching moment might have originated from a lift force in the vicinity of the booster fins. A test was therefore made with just the rear launching shoes in position, and the data (figs. 4 and 5) show that the negative pitching moment at 0° angle was the same as for the model with the hoisting lugs and launching shoes in place. This comparison indicated that the negative pitching moment was caused by the rear shoes.

The results of tests with the rear launching shoes faired are also shown in figures 4 and 5. Fairing the shoes eliminated the negative pitching moment at 0° angle of attack at a Mach number of 0.70, but at 0.85 Mach number the effect was only to reduce the negative pitching moment to about half what it was with the shoes unfaired.

To obtain a more complete understanding of the effect of the rear launching shoes, two rows of static-pressure orifices were installed on the alternate set of booster fins. The alternate booster fins differed geometrically from the standard fins (fig. 1); however, the interference effects of the launching shoes should be similar to those with the standard fins. Figure 9 is a plot for 0.85 Mach number of the pressure coefficients obtained at two spanwise stations from tests with and without the hoisting lugs and launching shoes in place. The decrease in the negative pressures on the lower surface forward of the shoes accounts for the positive lift and negative pitching moment.

Aerodynamic Characteristics of the Revised Model

As a compromise between the best aerodynamic design and the launching requirements, the shoes and lugs were faired and the rear shoes were moved forward of the fin leading edge. The two single hoisting lugs were changed to two double lugs and were placed diametrically opposite the launching shoes and made aerodynamically similar to the launching shoes. Figure 7 is a drawing and figure 10, a photograph showing the original and new shoe and lug positions.

The data for the revised model, using these launching-shoe and hoisting-lug positions on the long booster, are shown in figures 11 through 13. In general, there was no significant pitching moment or lift present at 0° angle of attack. A trim angle of about -0.5° existed throughout the Mach number range, as shown in figure 13. This small trim angle was probably due to slight misalinements of the model. The normal-force parameter as a function of Mach number (fig. 13) remained about constant up to a Mach number of 0.90, above which it increased slightly. The stability was slightly less than its low-speed value as the Mach number was increased up to 0.85, above which it decreased rapidly. The results of tests with various parts of the revised model removed are also shown in figures 11 through 13.

The results of changing the incidence on two diametrically opposite wings are shown in figures 14 through 16. The normal-force characteristics shown in figure 14 for wing incidences of 2° and 4° with the fins in the normal position, and 4° with the fins rolled 45°, are the same as those for 0° wing incidence except for a small decrease in the angle of attack for zero lift. The stability was the same for all the wing-incidence tests at normal-force coefficients near zero. The stability increased rapidly above a normal-force coefficient of about 4.5 for the 2° wing incidence, and increased rapidly above a normal-force coefficient of about 2.5 for the 4° wing incidence. The trim angles as a function of Mach number for the various wing incidences are shown in figure 16. The trim angle increased roughly 2° for each 2° increase in wing incidence. The trim angle increased throughout the Mach number range. Rolling the booster fins 45° had little effect on the trim angle.

Since the cause of the flight failures was originally thought to be lack of stability, the model was fitted so that various methods for increasing the stability could be investigated. Even though it was found that lack of stability was not the cause of the flight failures, tests of these methods for increasing the stability were made and are reported in the remainder of this discussion. The results of tests of spoilers on the wings (fig. 17) are shown in figures 18 and 19. The normal-force results (fig. 18) are similar to the results without spoilers except for a slight decrease in the normal-force parameter. The stability was increased except at the low Mach numbers and small angles of attack.

Data for tests with the missile rolled 22.5° relative to the booster so that the missile tails were in line with the booster fins are shown in figures 20 and 21. The normal-force data were not altered by the change except for a slight decrease in the normal-force parameter, which was probably caused by the change in the tail wake acting on the booster fins. The stability was about the same for both conditions.

Data for the complete model, including the booster rolled 45° and 90°, are shown in figures 22 through 24. The normal-force parameters for the model in the rolled positions increased with increasing Mach number. For the 45° position, however, at 0.9 Mach number, the normal-force parameter for this position decreased to below that for 0° roll as shown in figure 24. The stability parameter as a function of Mach number (fig. 24) for the 45° roll was about the same as for the 0° position up to a Mach number of 0.85°, above which the stability increased. The stability for the 90° position decreased throughout the Mach number range, decreasing more rapidly above 0.85 Mach number.

The results of tests with the alternate booster fins are shown in figures 25 and 26. The dimensions of the fins are shown in figure 1. The normal-force and stability parameters are shown as a function of Mach number in figure 27. The stability for the model with the alternate booster fins was greater than with the standard fins by an amount corresponding to a neutral-point shift of 6 percent of the total missile length. There was little change in stability with Mach number up to 0.88, above which the stability decreased rapidly. The normal-force parameter was increased an average of about 20 percent with the use of alternate booster fins.

CONCLUDING REMARKS

It was concluded that the failures of the booster fins on the Bumblebee missile were due to launching shoes which caused the missile to trim at increasing negative angles of attack as the Mach number increased. Under these conditions, the booster fins apparently became overloaded to the point of failure. (Subsequent to the tests reported herein, it has been determined that the torsional deflection of the missile wings also contributed to the failure of the booster fins.)

A design was developed for the launching shoes and hoisting lugs which eliminated the adverse effect on the pitching moment. It consisted of faired shoes and lugs, with rear shoes moved forward of the fin leading edge. The single hoisting lugs were changed to double lugs placed diametrically opposite the shoes and made aerodynamically similar to the launching shoes.

Wing spoilers were effective in increasing the stability except at low Mach numbers and small angles of attack.

The alternate booster fins increased the stability by an amount equal to a neutral point shift of 6 percent of the total missile length.

Ames Aeronautical Laboratory,
National Advisory Committee for Aeronautics,
Moffett Field, Calif.

REFERENCE

1. Herriot, John G.: Blockage Corrections for Three-Dimensional-Flow Closed-Throat Wind Tunnels, With Consideration of the Effect of Compressibility. NACA RM A7B28, 1947.

[redacted]

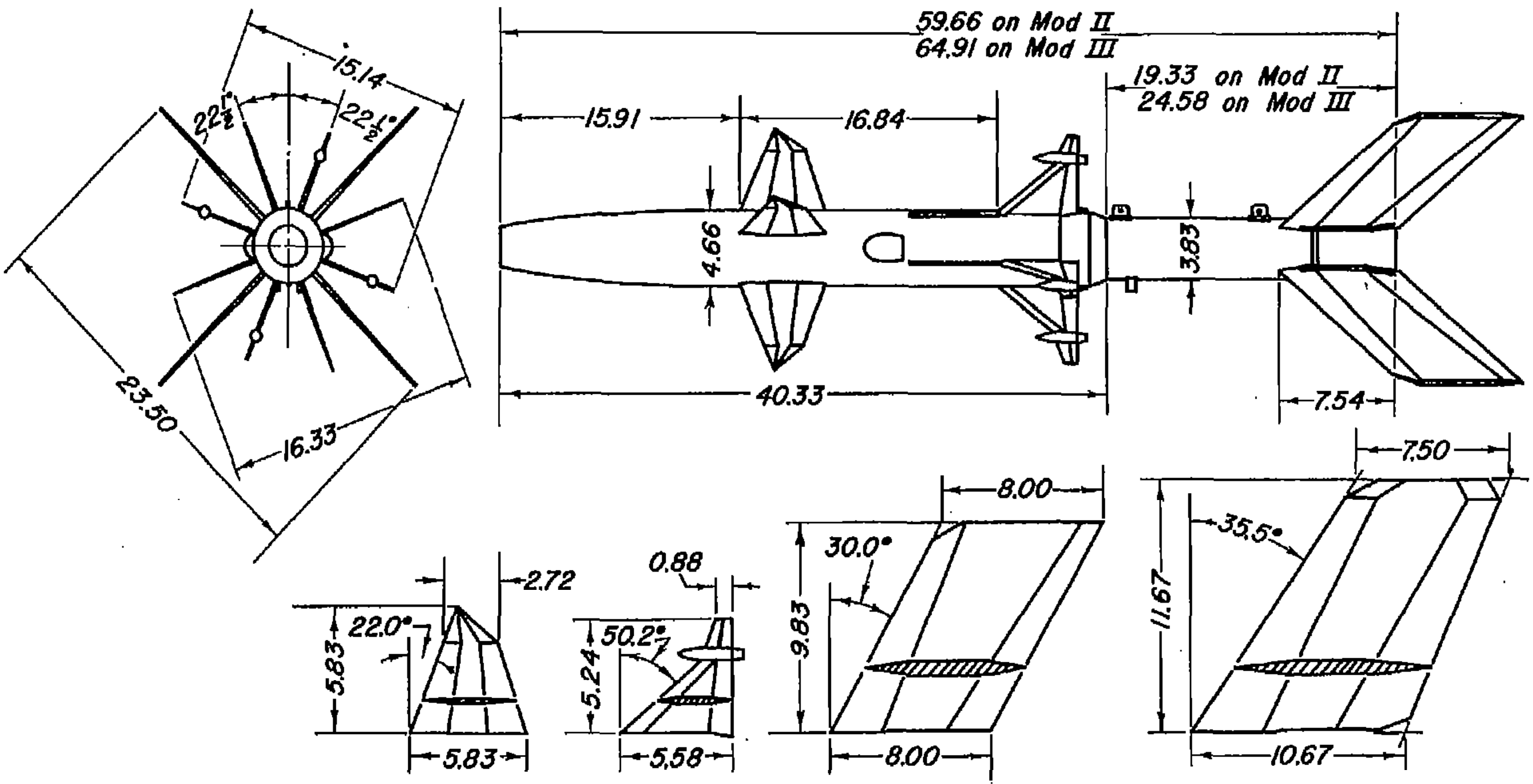

	Wing	Tail	Standard booster fin	Alternate booster fin
Root thickness, % chord	5.0	6.0	10.0	7.0
Tip thickness, % chord	3.0	7.5	5.0	4.4

Note: All dimensions in inches.

Figure 1.– Dimensions of model and component parts.

[redacted]

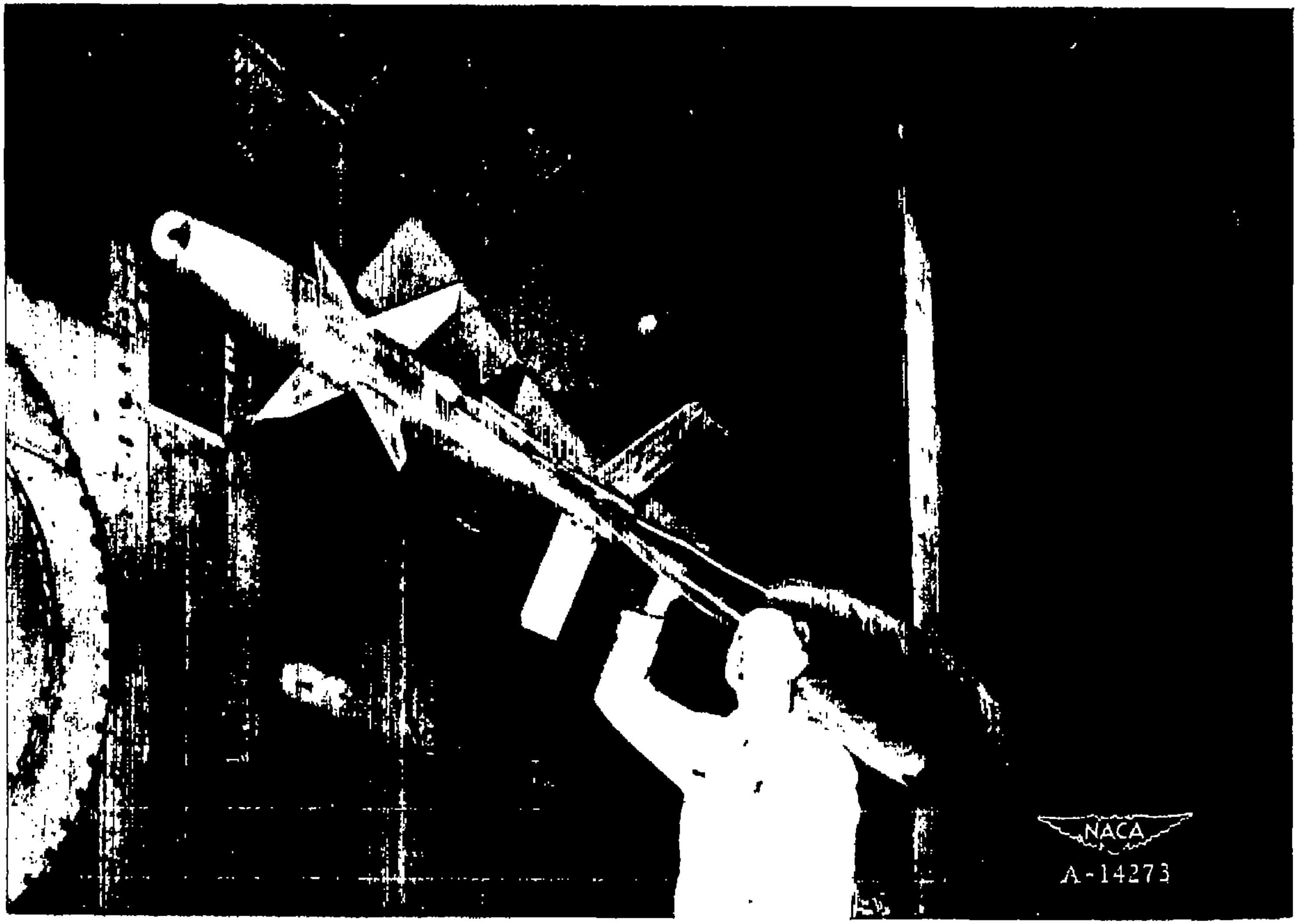

Figure 2.– Photograph of the model mounted on the sting.

[redacted]

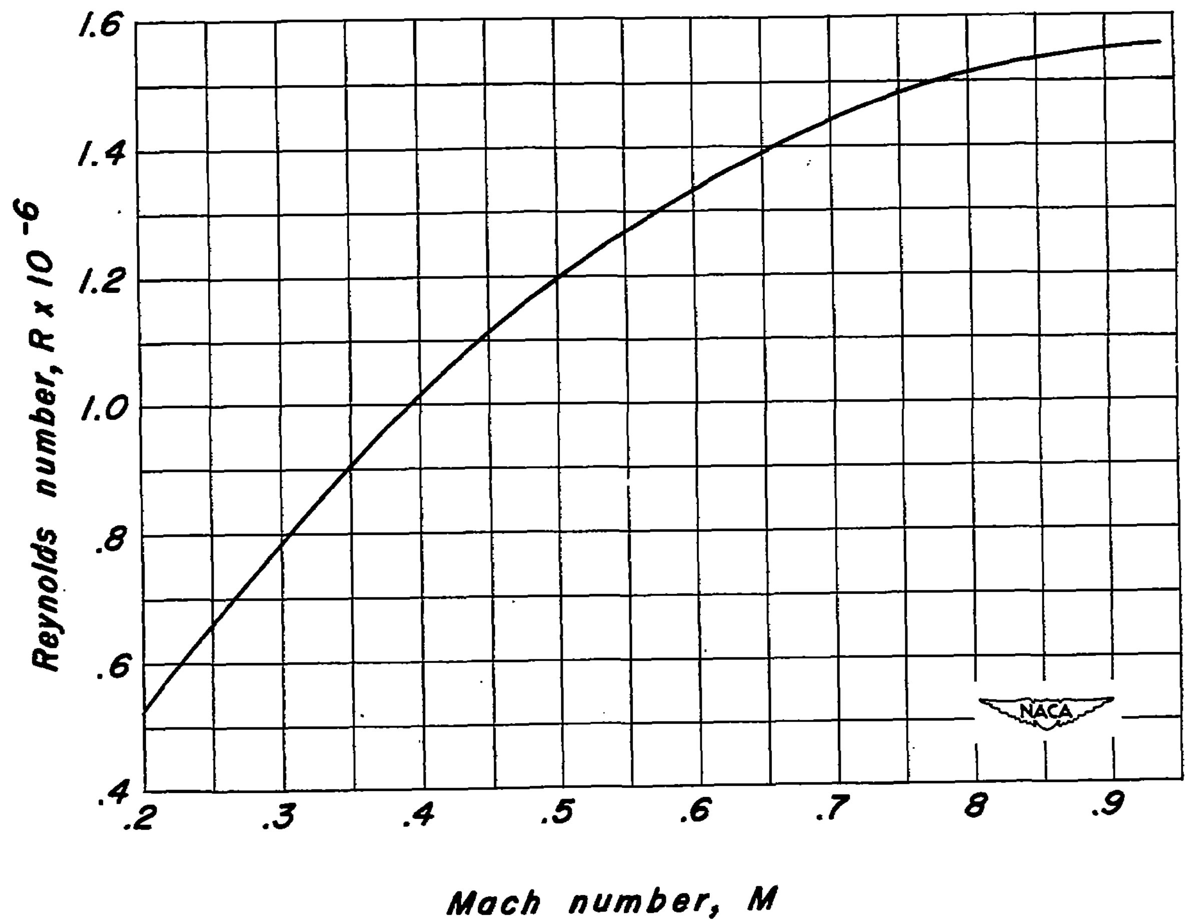

Figure 3.—Variation of the average Reynolds number with Mach number.

[redacted]

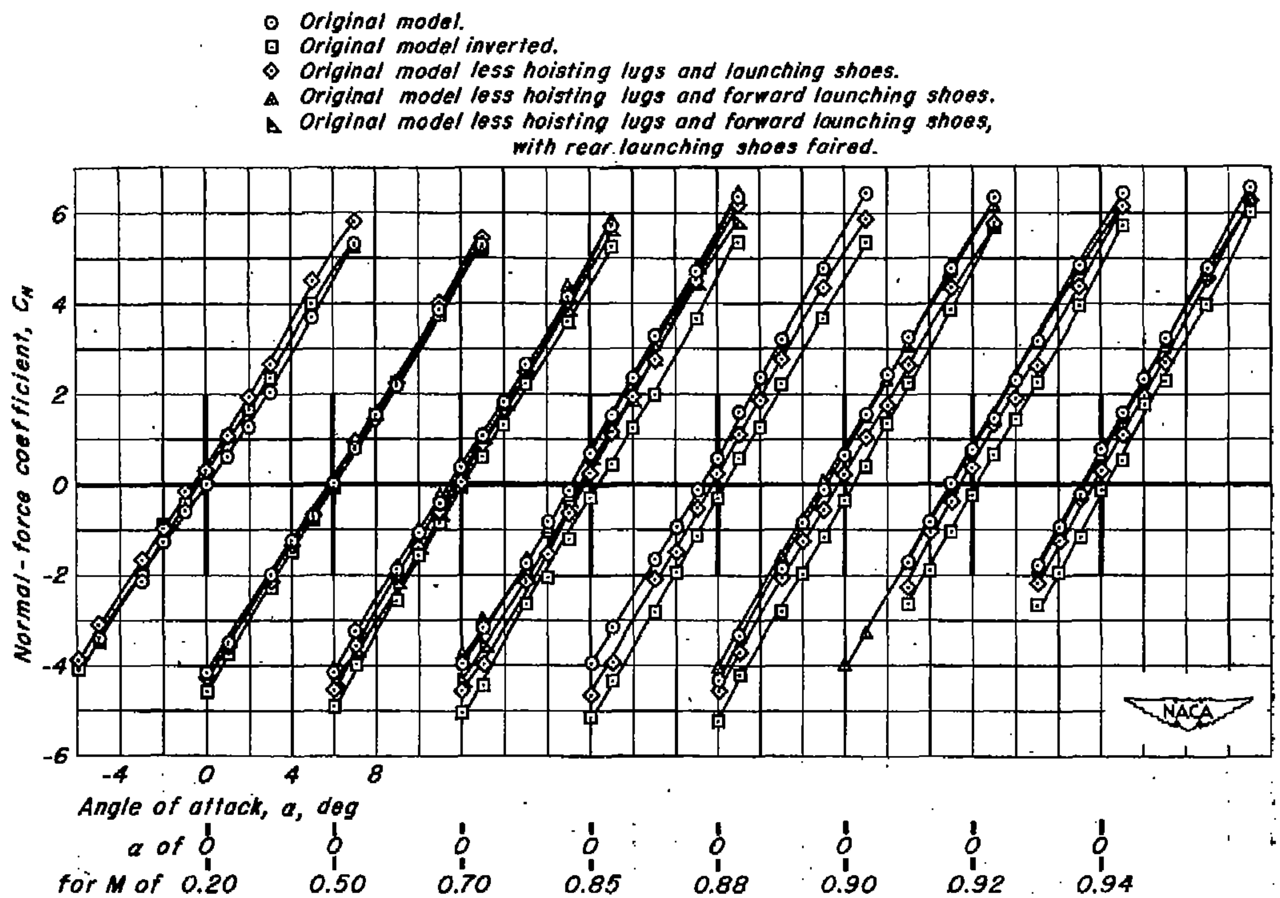

Figure 4.– Variation of normal-force coefficient with angle of attack for the original model with different hoisting lug and launching shoe arrangements.

[redacted]

[redacted]

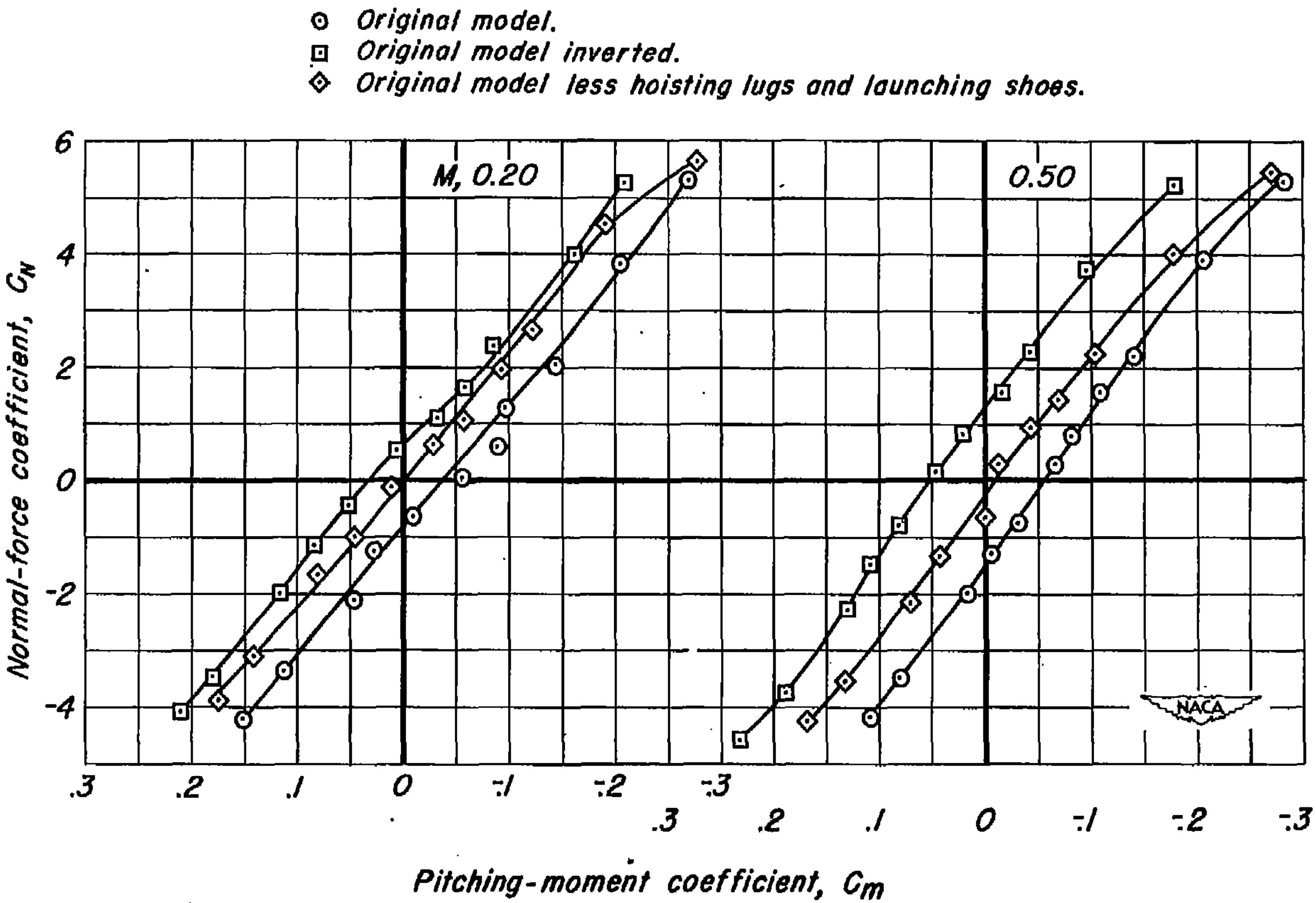

(a) M, 0.20, 0.50.

Figure 5.– Variation of normal-force coefficient with pitching-moment coefficient for the original model with different hoisting lug and launching shoe arrangements.

[redacted]

[redacted]

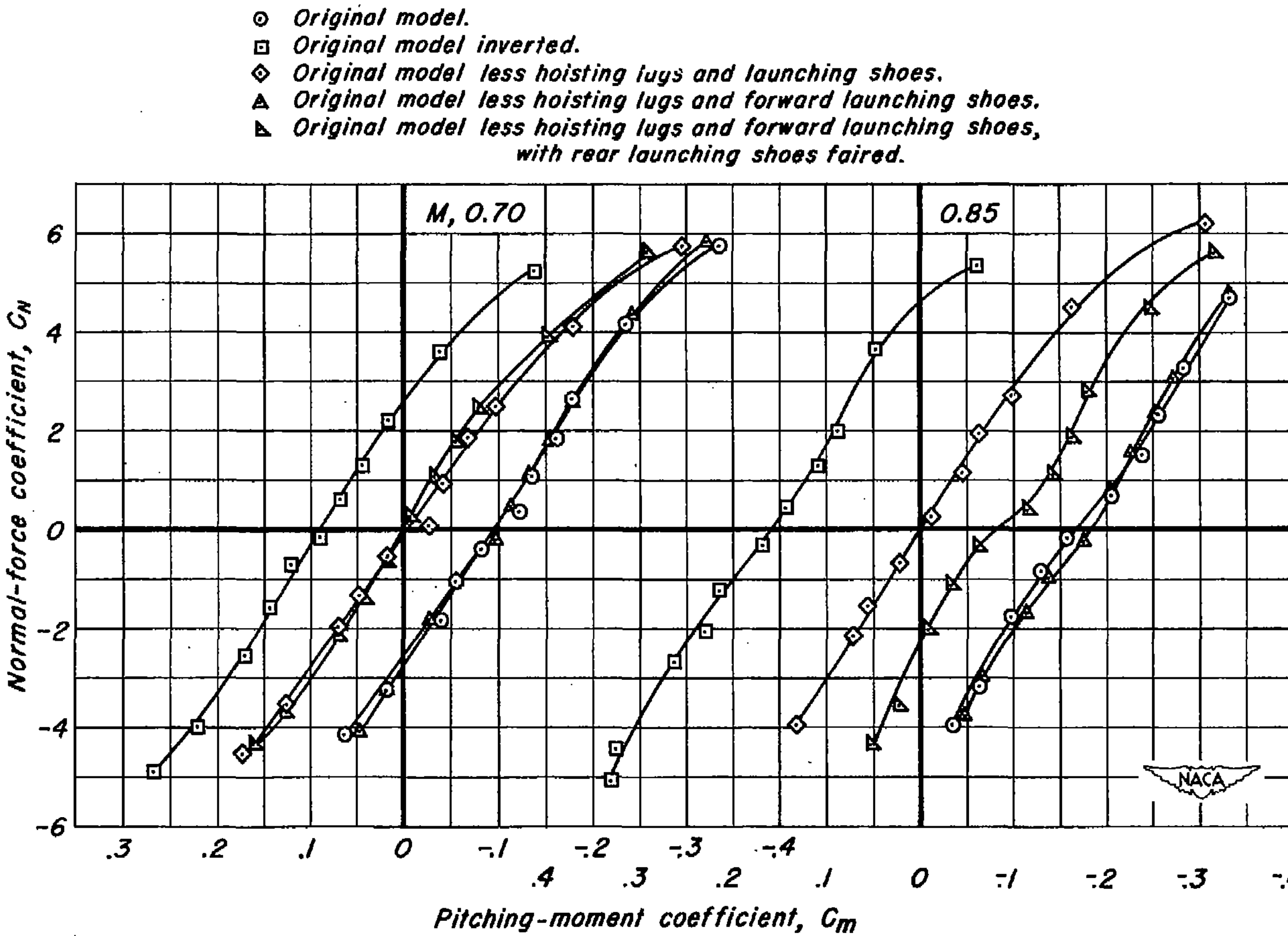

(b) M, 0.70, 0.85.

Figure 5.— Continued.

[redacted]

[redacted]

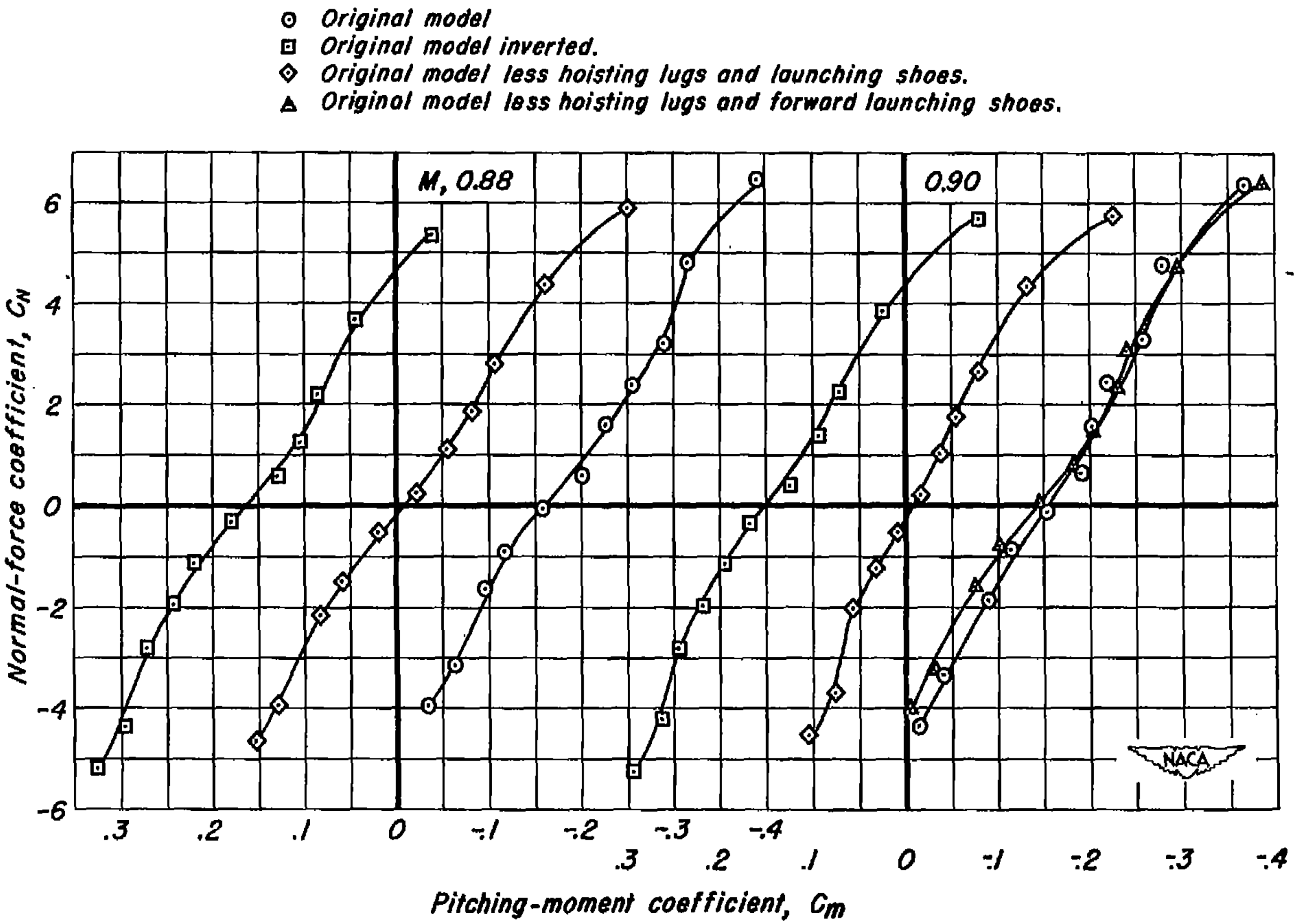

(a) M, 0.88, 0.90.

Figure 5.— Continued.

[redacted]

[redacted]

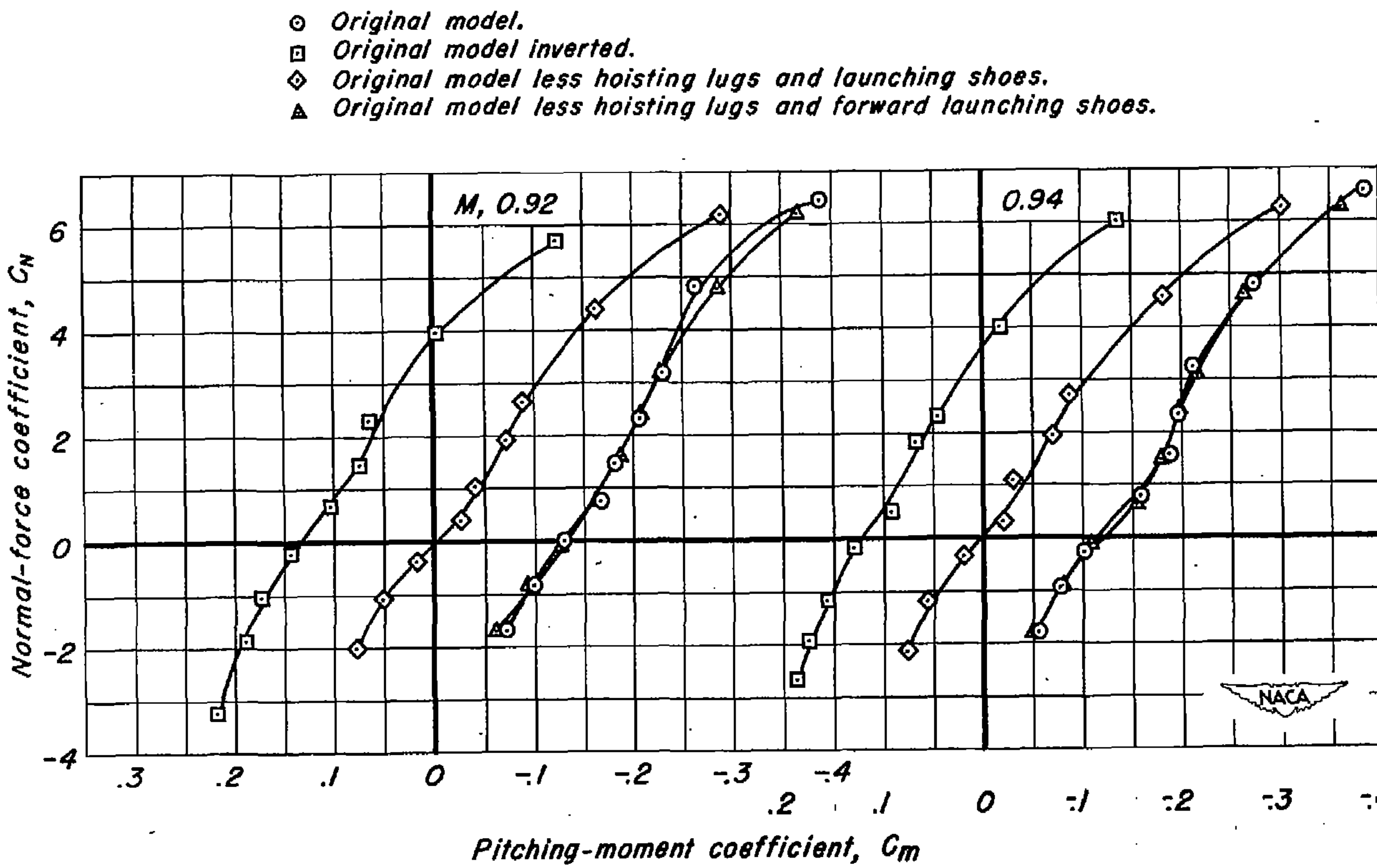

(d) M, 0.92, 0.94.

Figure 5.— Concluded.

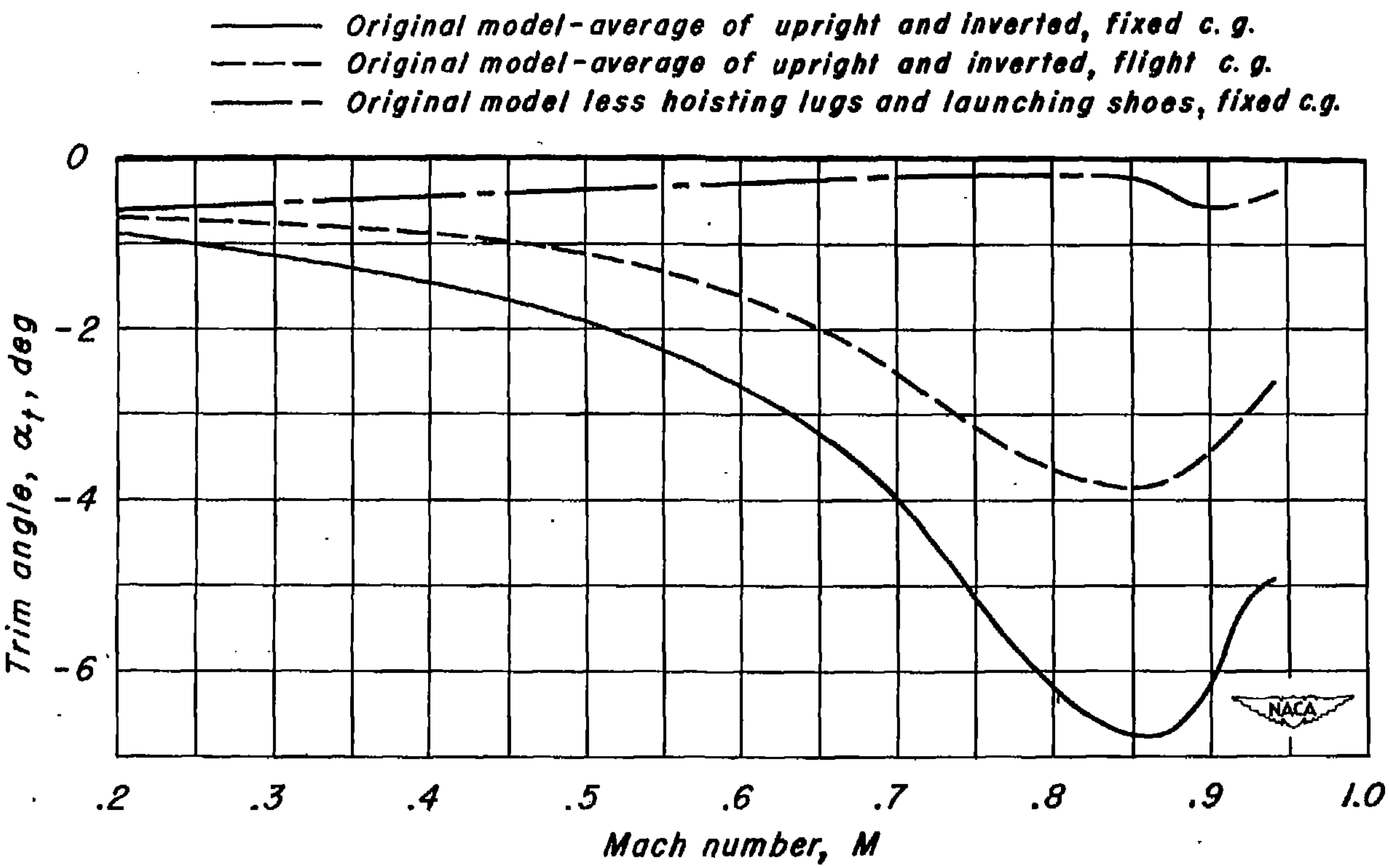

Figure 6.—Variation of trim angle with Mach number for the original model.

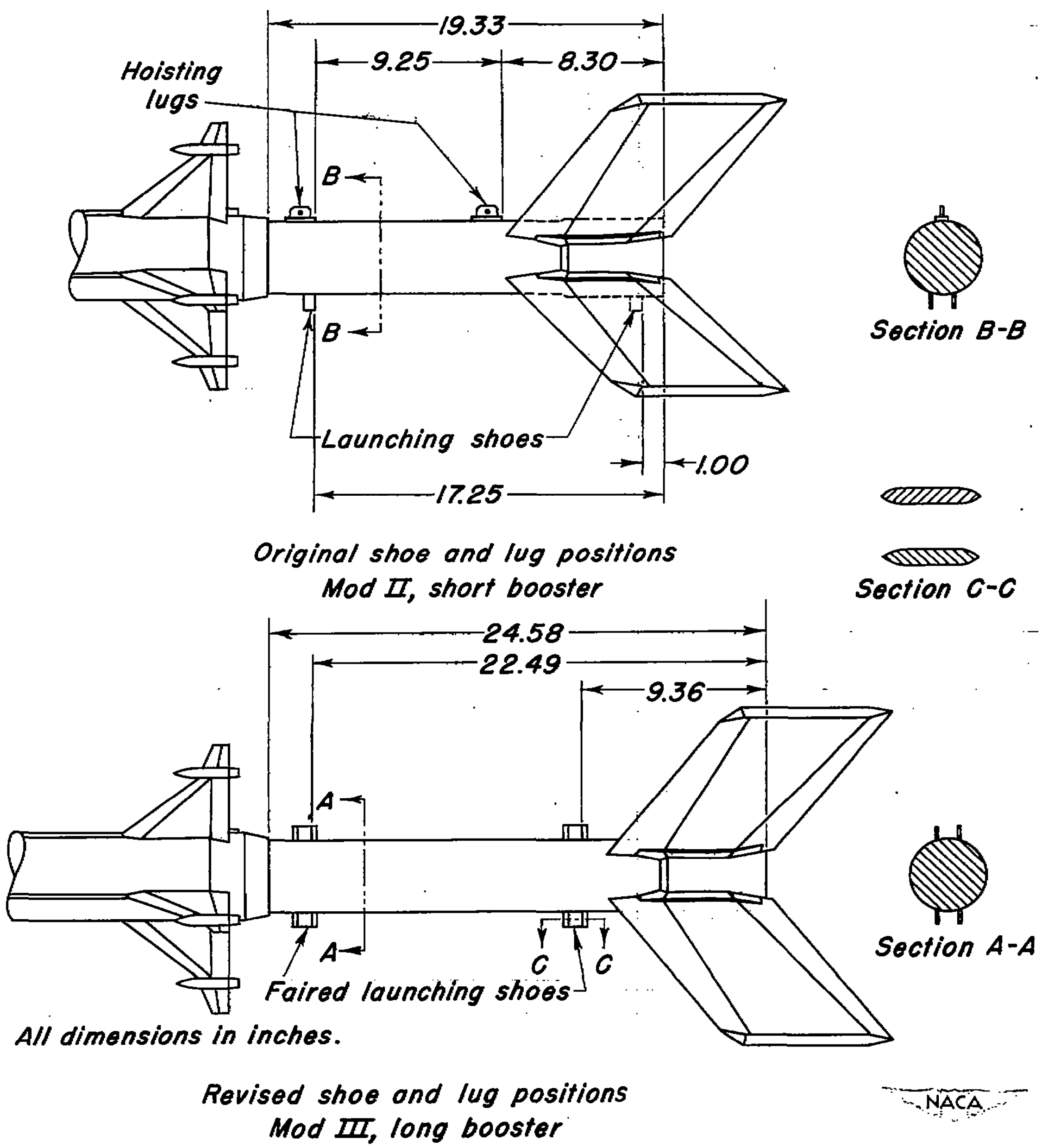

Figure 7.– Shoe and lug positions on the original and revised model.

[redacted]

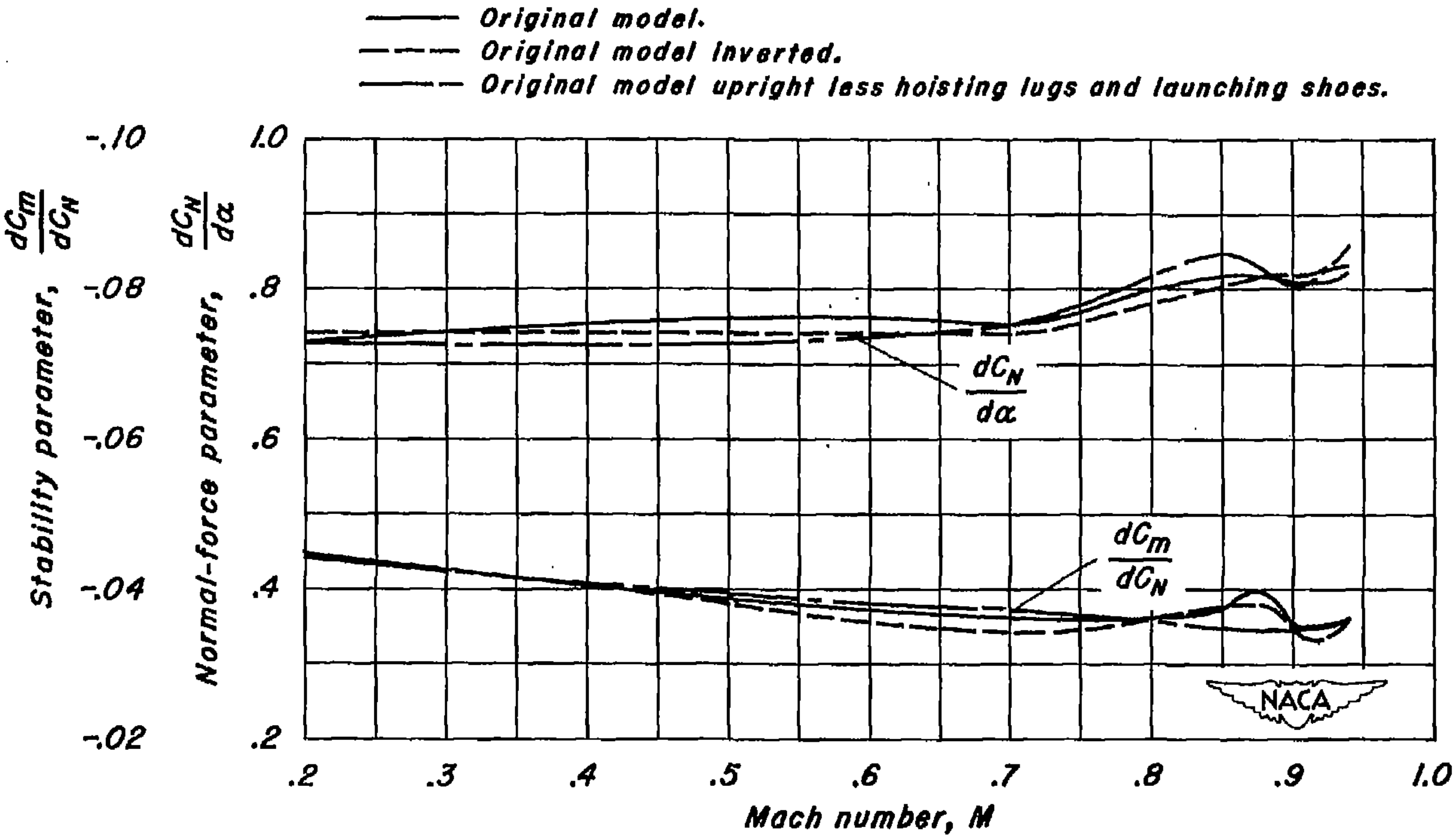

Figure 8.—Variation of normal-force and stability parameters with Mach number for the original model.

[redacted]

[redacted]

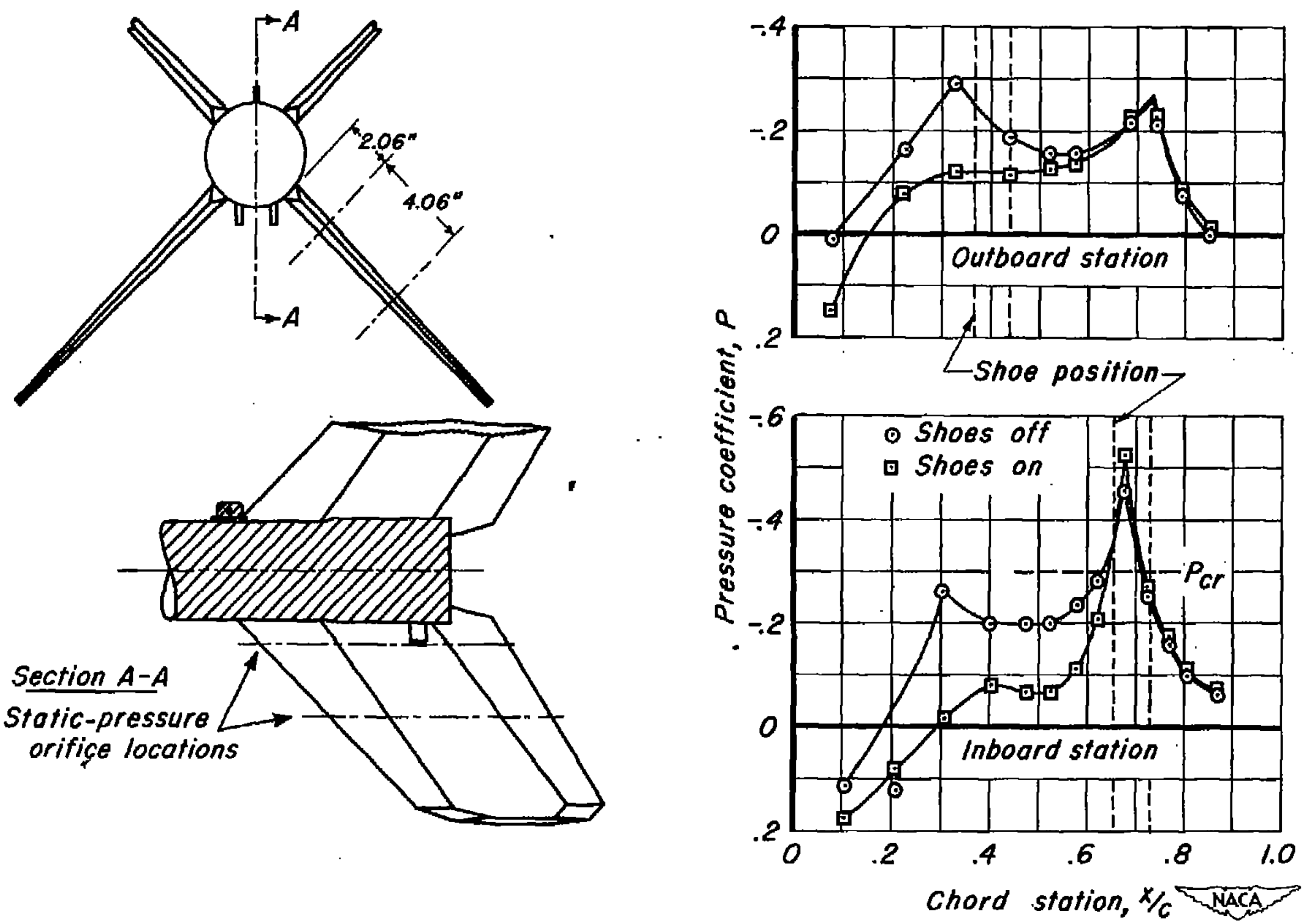

Figure 9.–Chordwise pressure distributions on the lower surface of the alternate booster fins. α, 0°; M, 0.85.

[redacted]

[redacted]

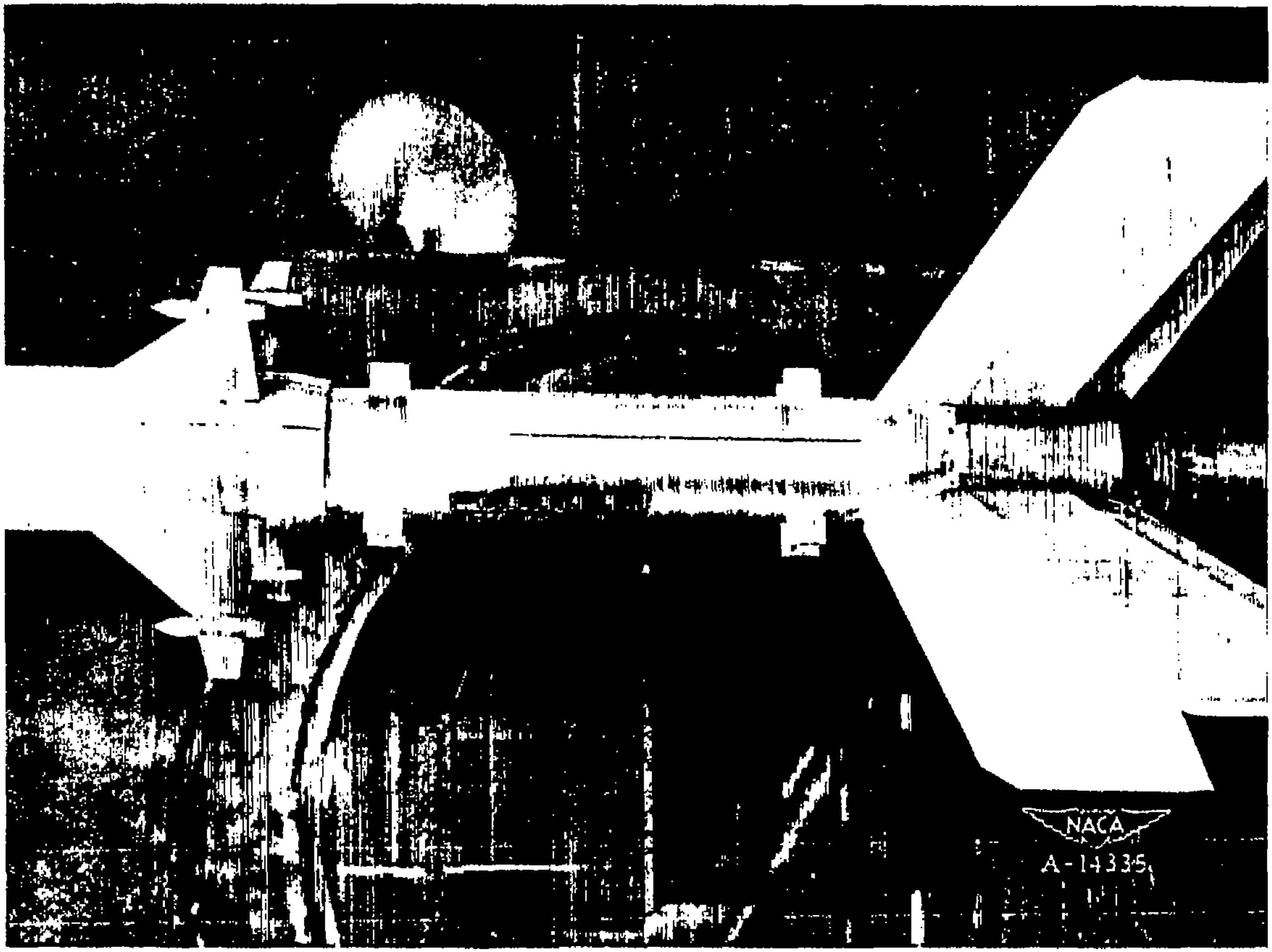

Figure 10.— Photograph of the final launching shoe positions.

[redacted]

[redacted]

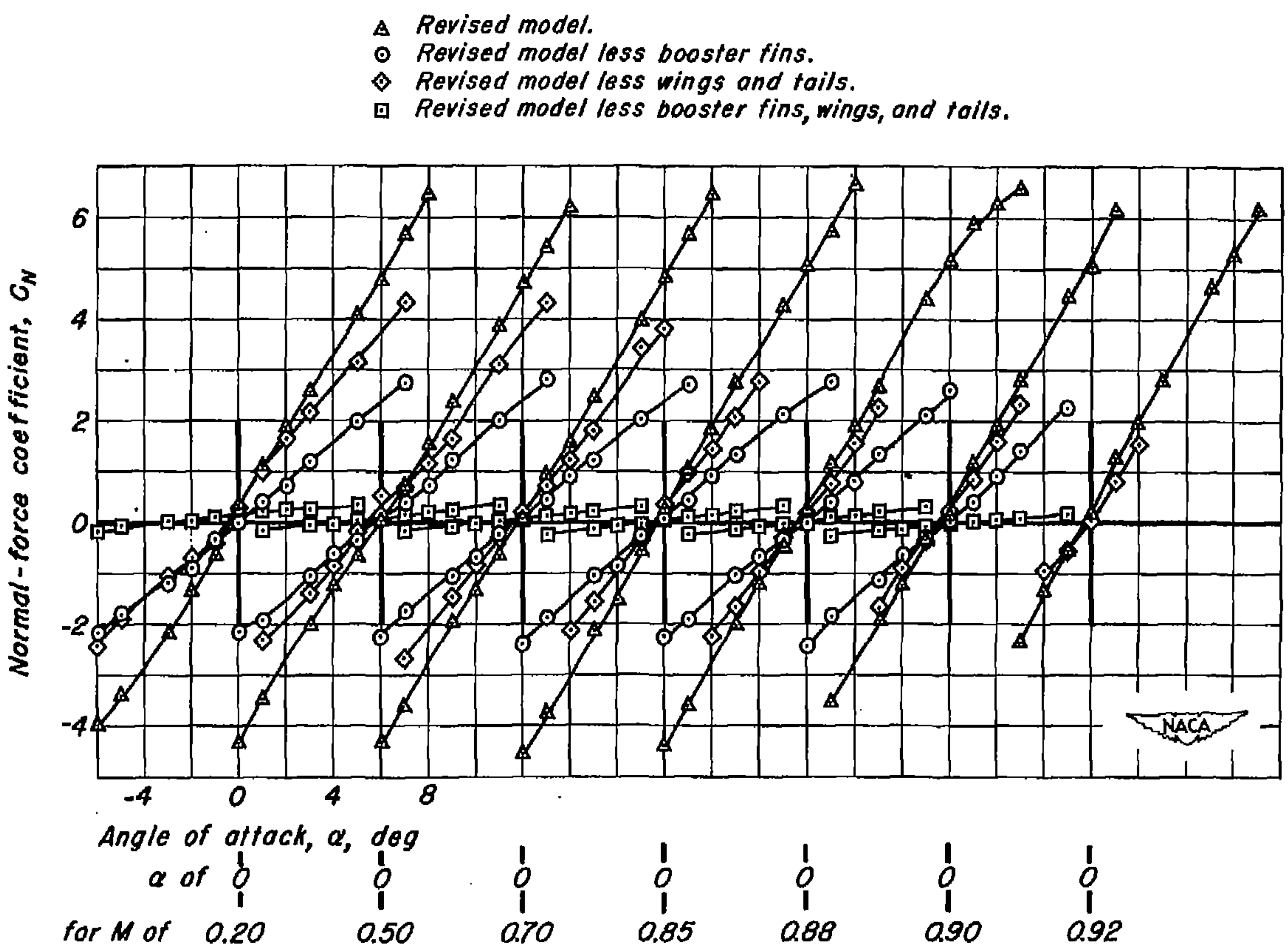

Figure 11.–Variation of normal-force coefficient with angle of attack for the revised model.

[redacted]

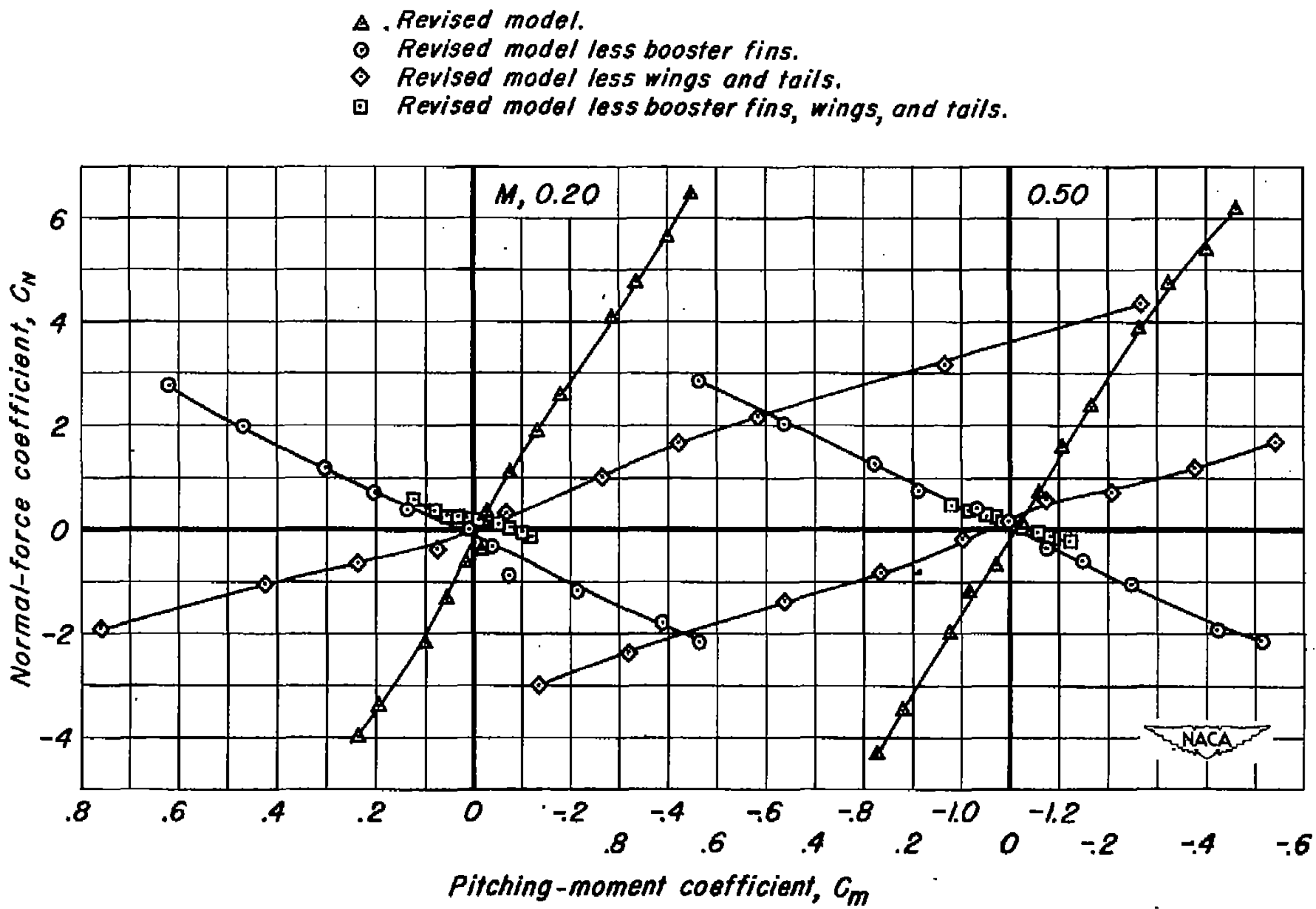

(a) M, 0.20, 0.50.

Figure 12.—Variation of normal-force coefficient with pitching-moment coefficient for the revised model.

[redacted]

[redacted]

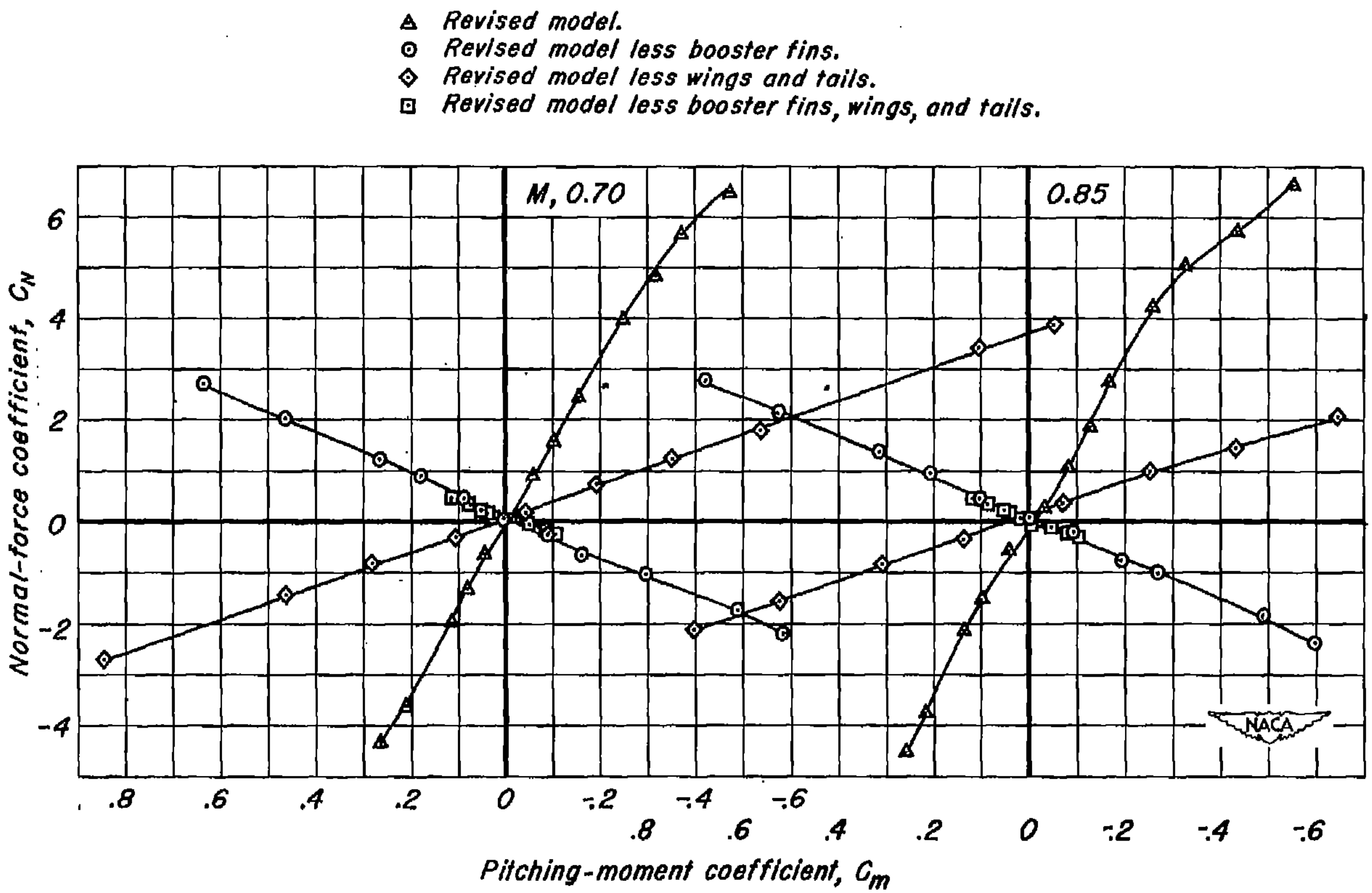

(b) M, 0.70, 0.85.

Figure 12.–Continued.

[redacted]

[redacted]

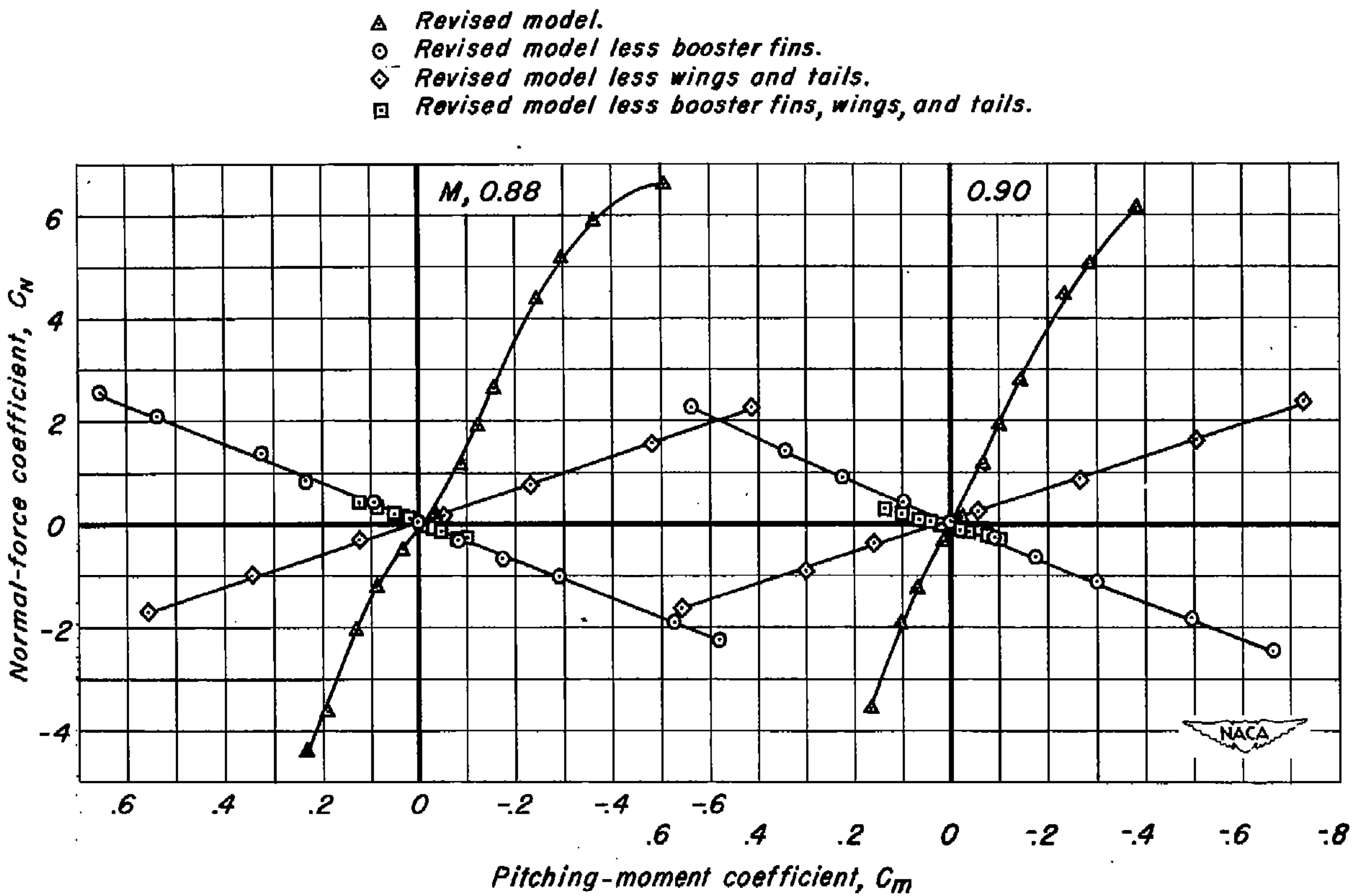

(c) M, 0.88, 0.90.

Figure 12.—Continued.

[redacted]

[redacted]

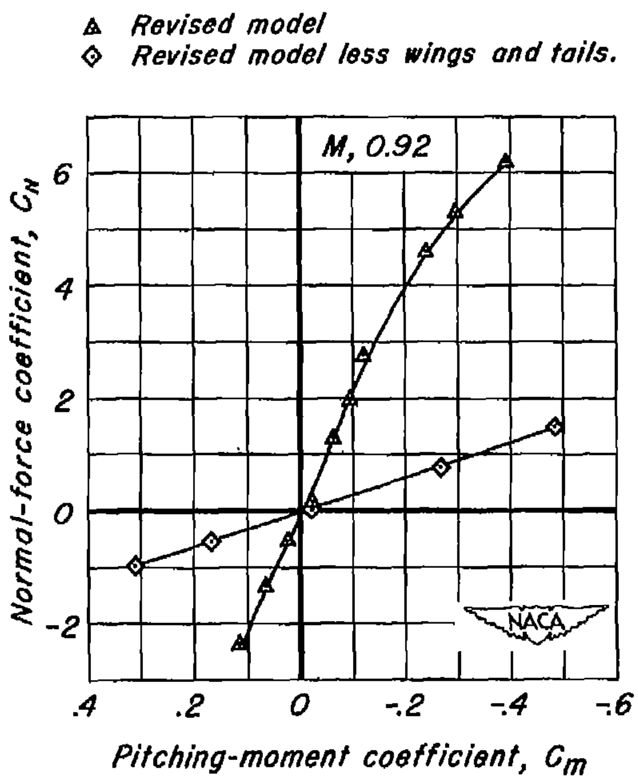

(d) M, 0.90.

Figure 12.– Concluded.

[redacted]

[redacted]

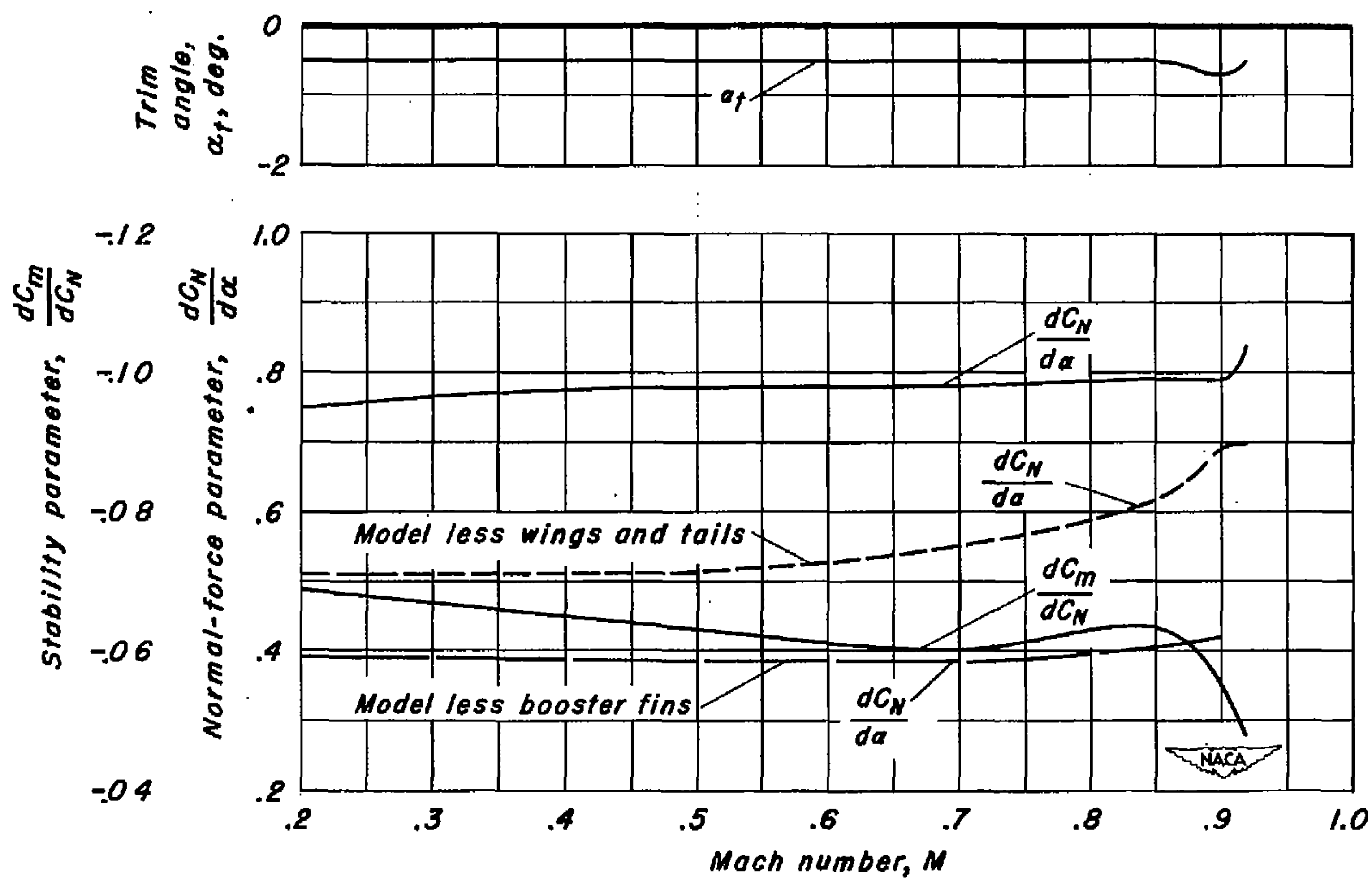

Figure 13.–Variation of normal-force and stability parameters with Mach number for the revised model.

[redacted]

[redacted]

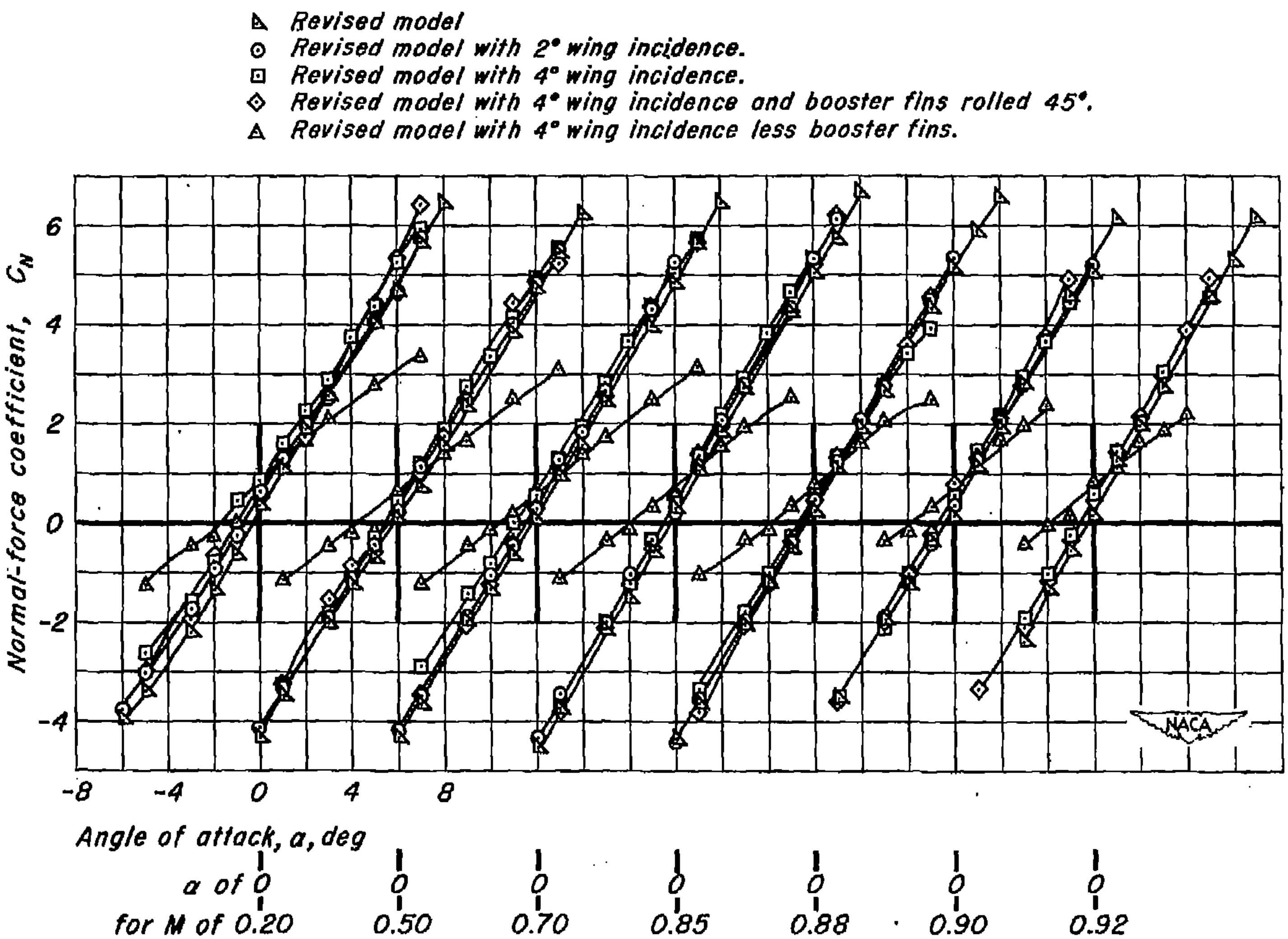

Figure 14.–Variation of normal-force coefficient with angle of attack for the revised model with various wing incidences.

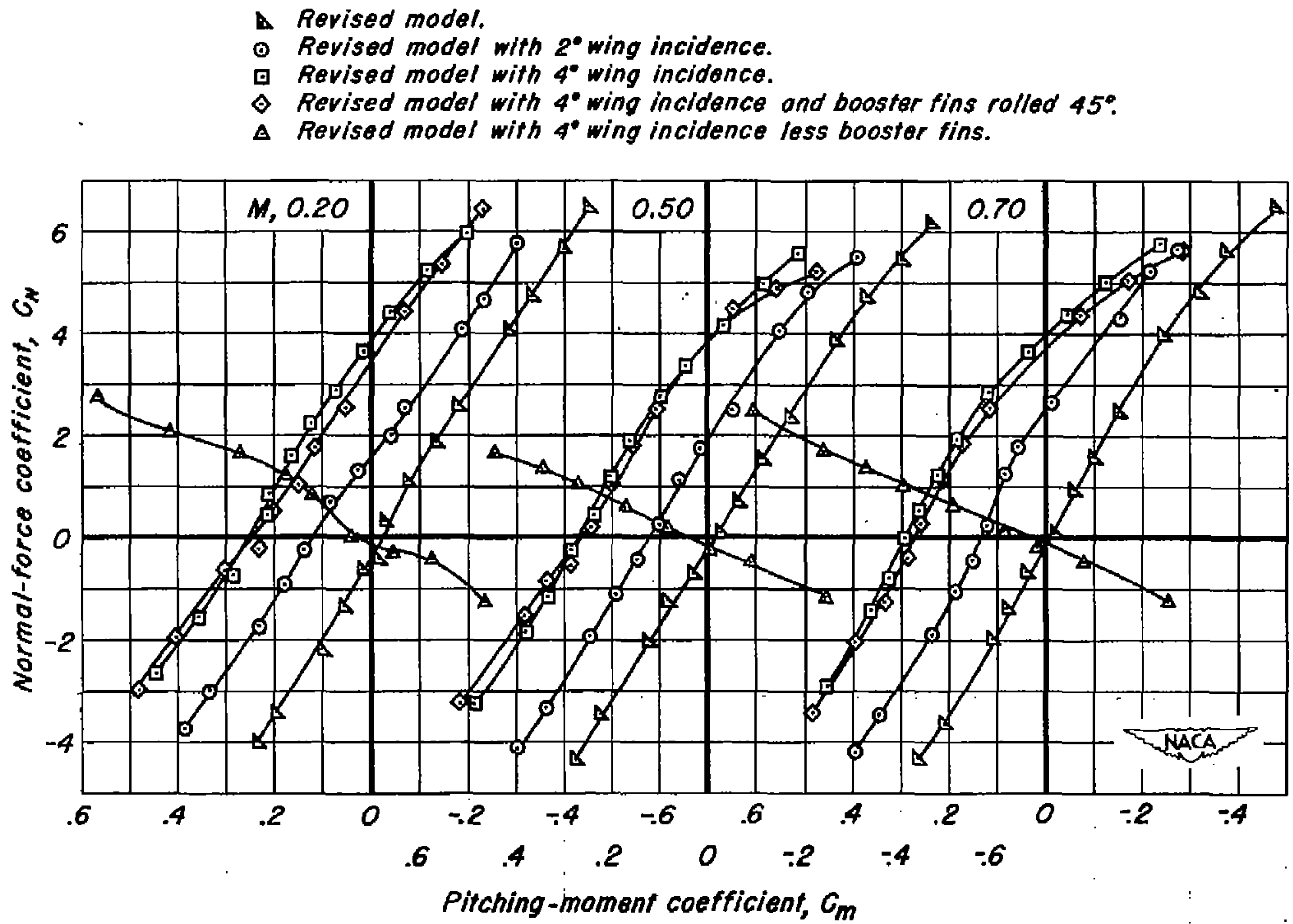

(a) M, 0.20, 0.50, 0.70.

Figure 15.—Variation of normal-force coefficient with pitching-moment coefficient for the revised model with various wing incidences.

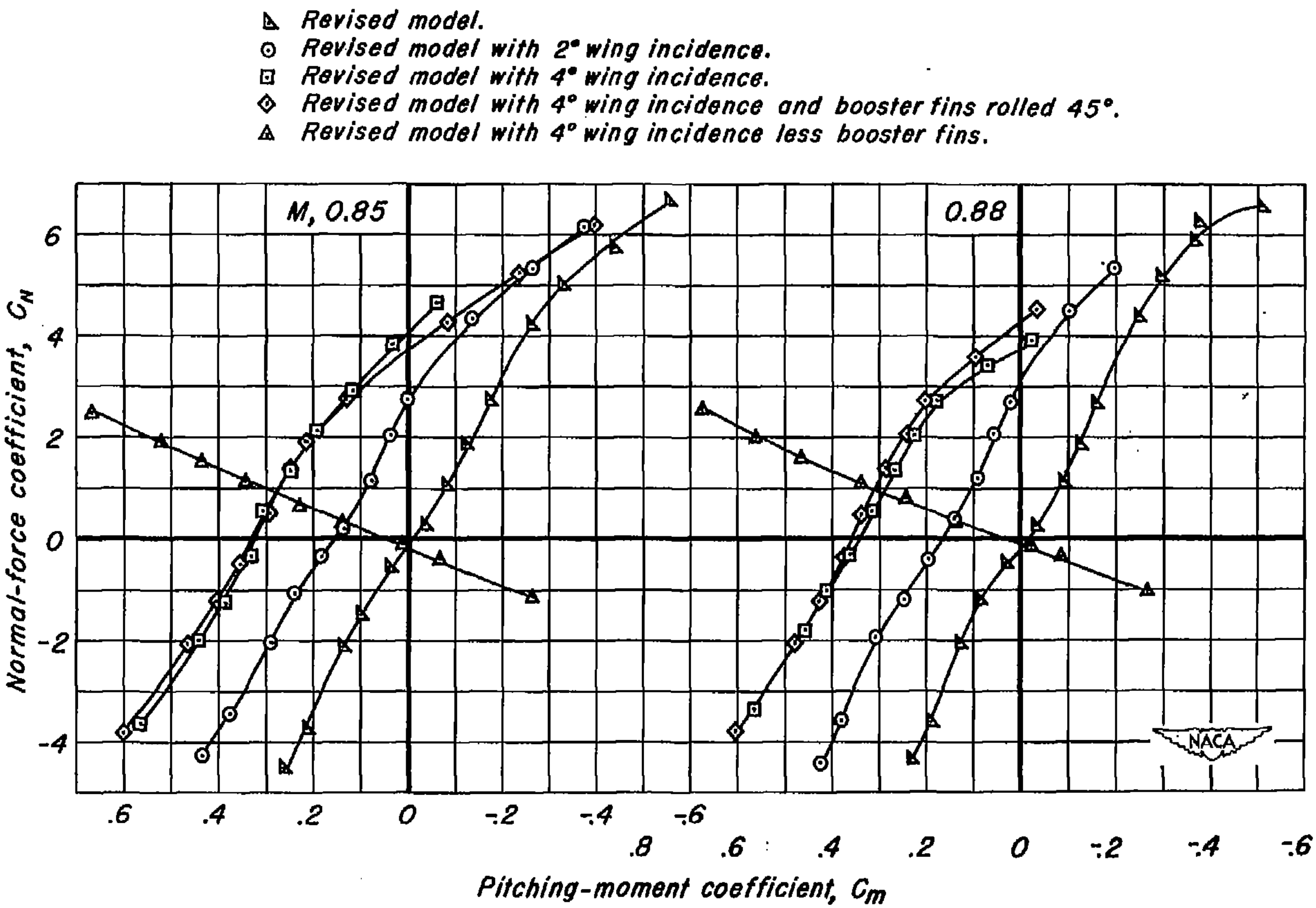

(b) M, 0.85, 0.88.

Figure 15.—Continued.

[redacted]

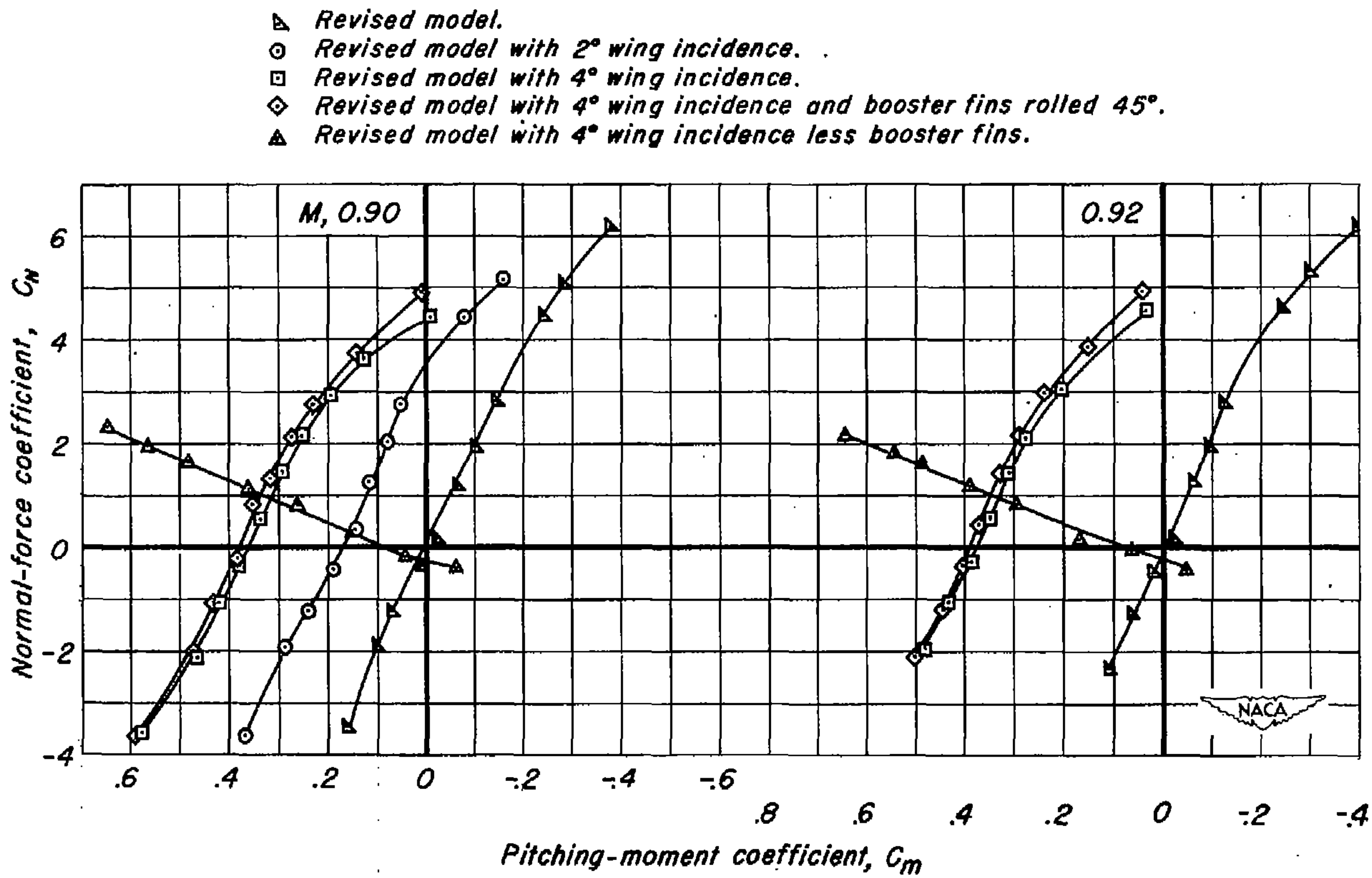

(c) M, 0.90, 0.92.

Figure 15.—Concluded.

[redacted]

[redacted]

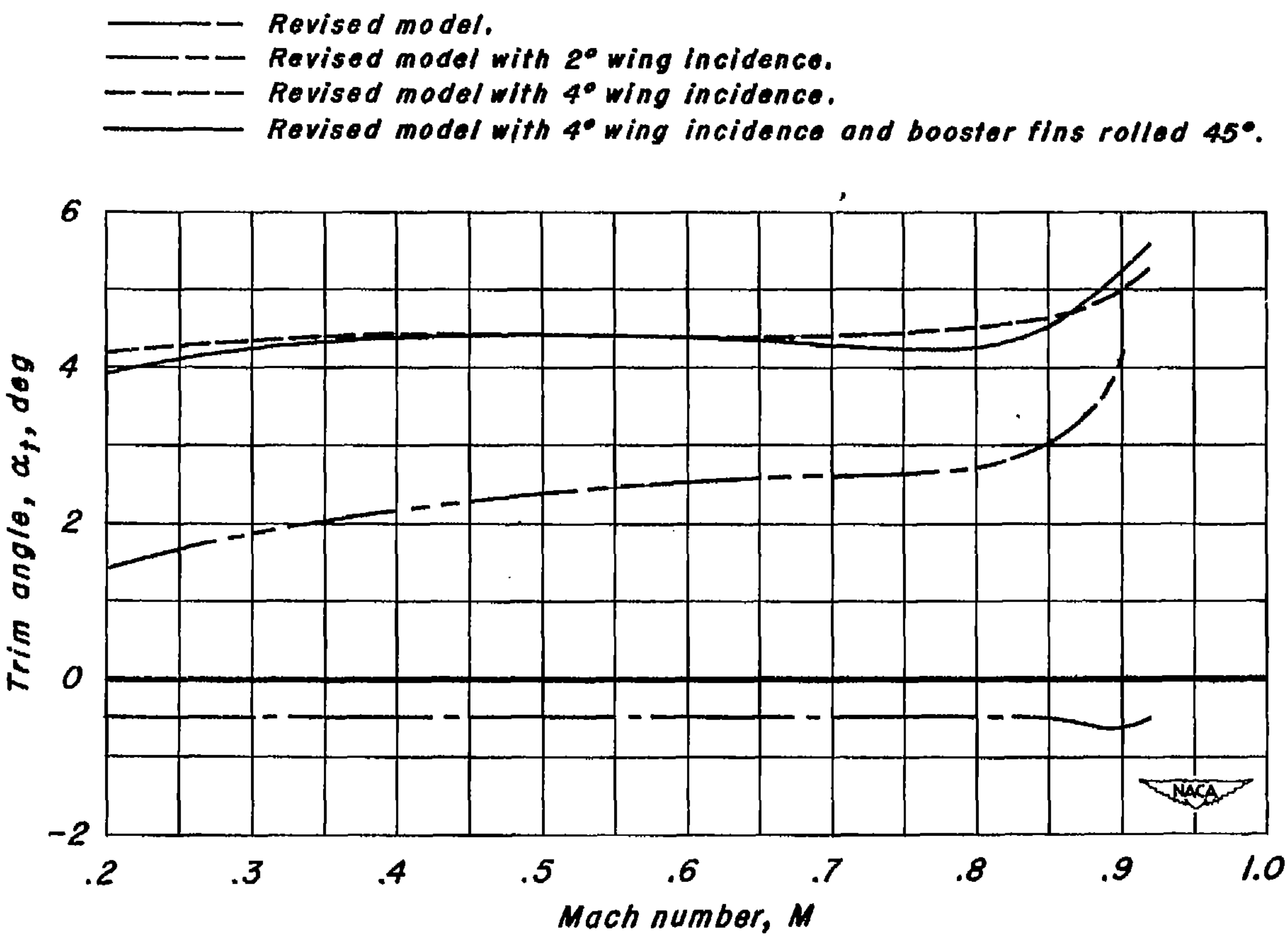

Figure 16.—Variation of trim angle with Mach number for the revised model with various wing incidences.

[redacted]

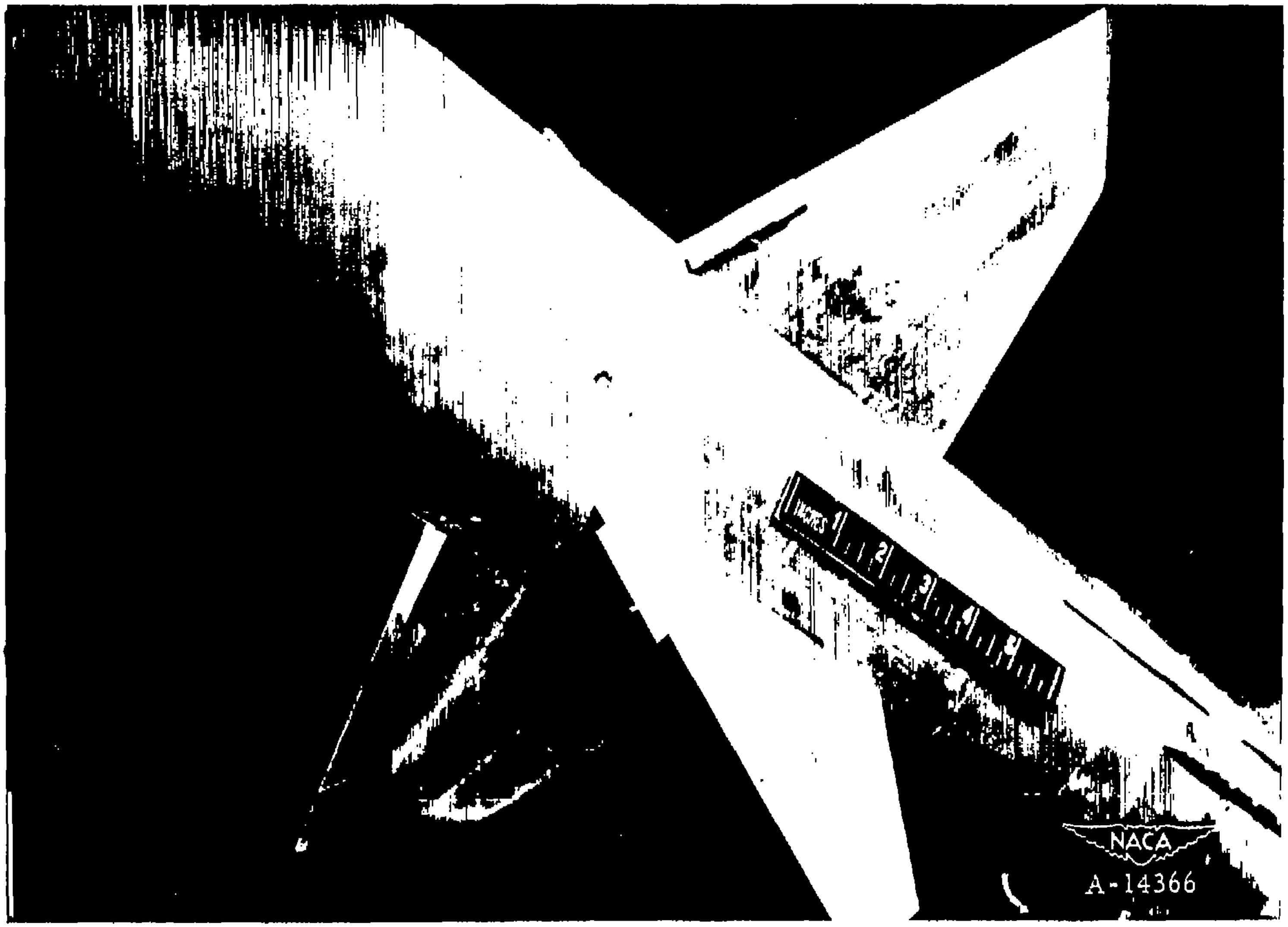

Figure 17.– Photograph of the spoilers mounted on the wings.

[redacted]

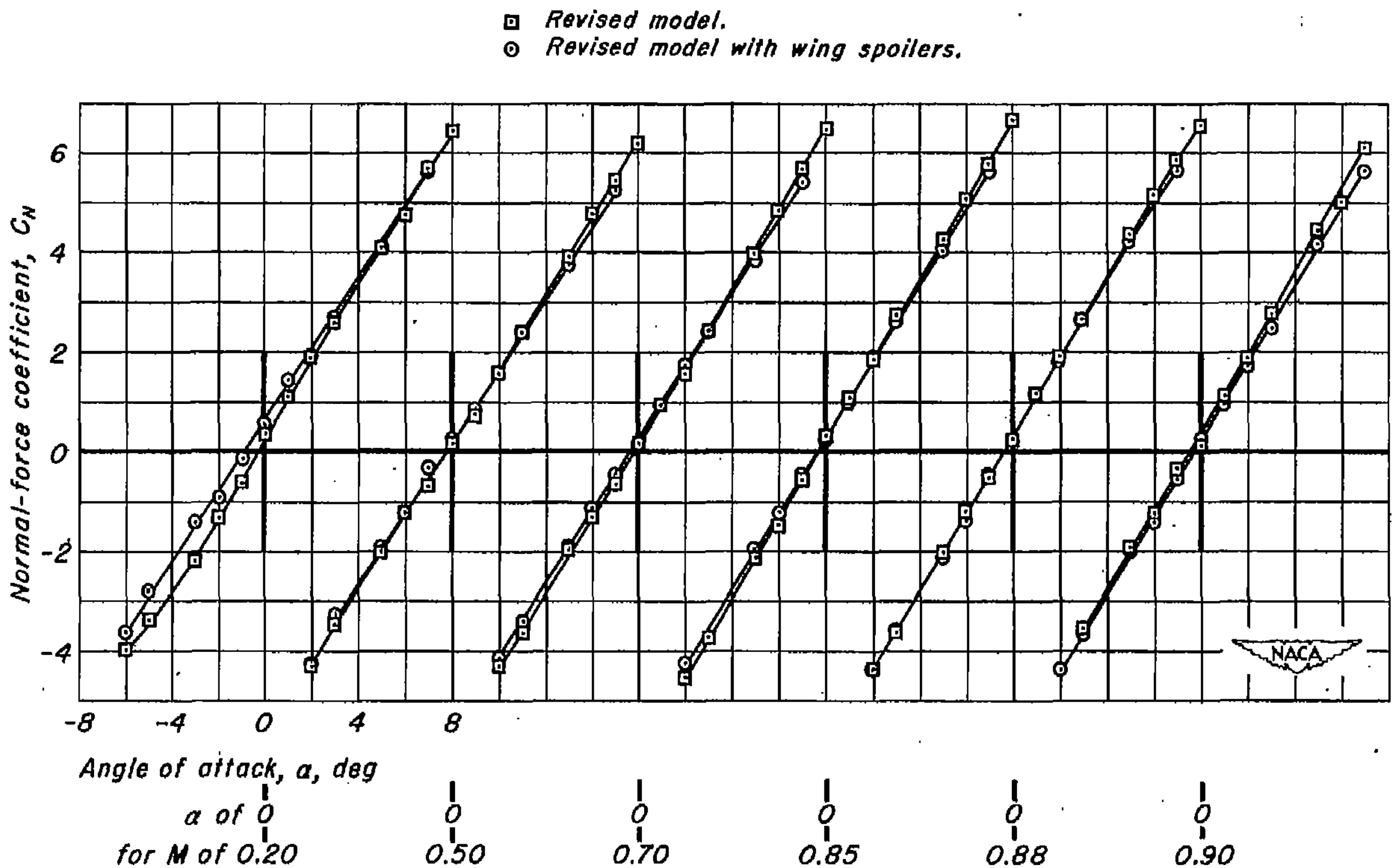

Figure 18.– Variation of normal-force coefficient with angle of attack for the revised model with wing spoilers.

[redacted]

[redacted]

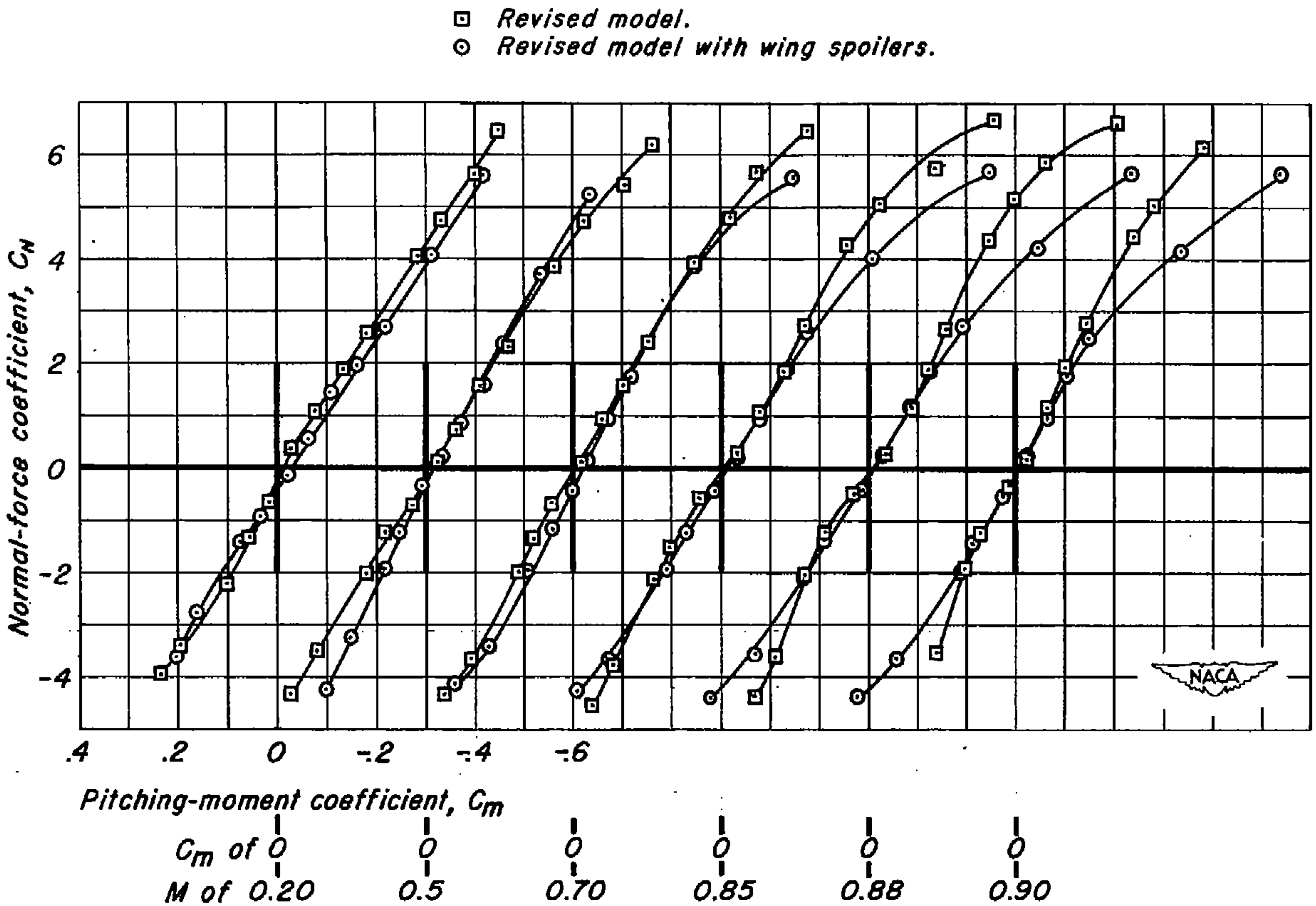

Figure 19.–Variation of normal-force coefficient with pitching moment coefficient for the revised model with wing spoilers.

[redacted]

[redacted]

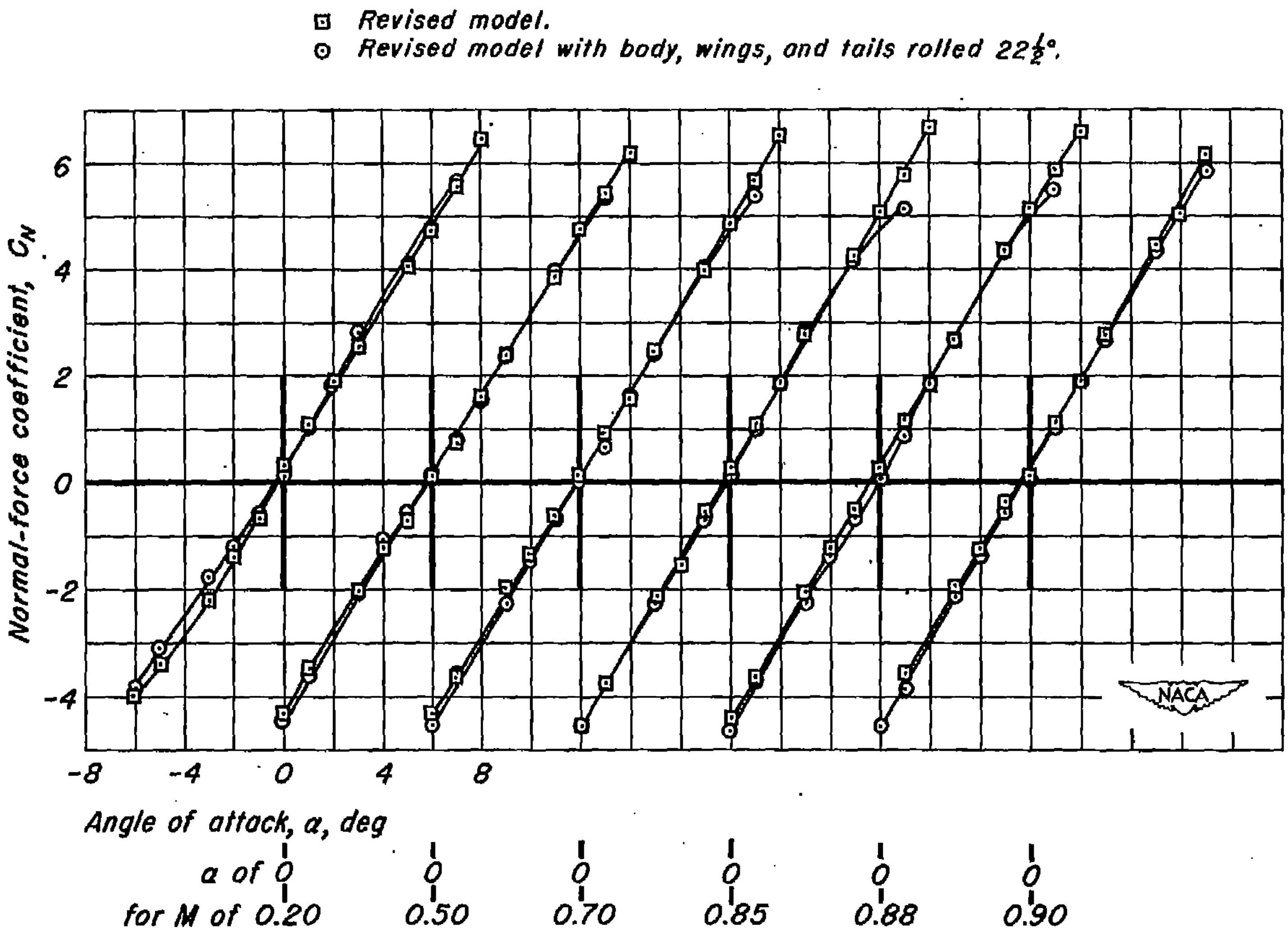

Figure 20.–Variation of normal-force coefficient with angle of attack for the revised model with the body, wings and tails rolled 22½°.

[redacted]

[redacted]

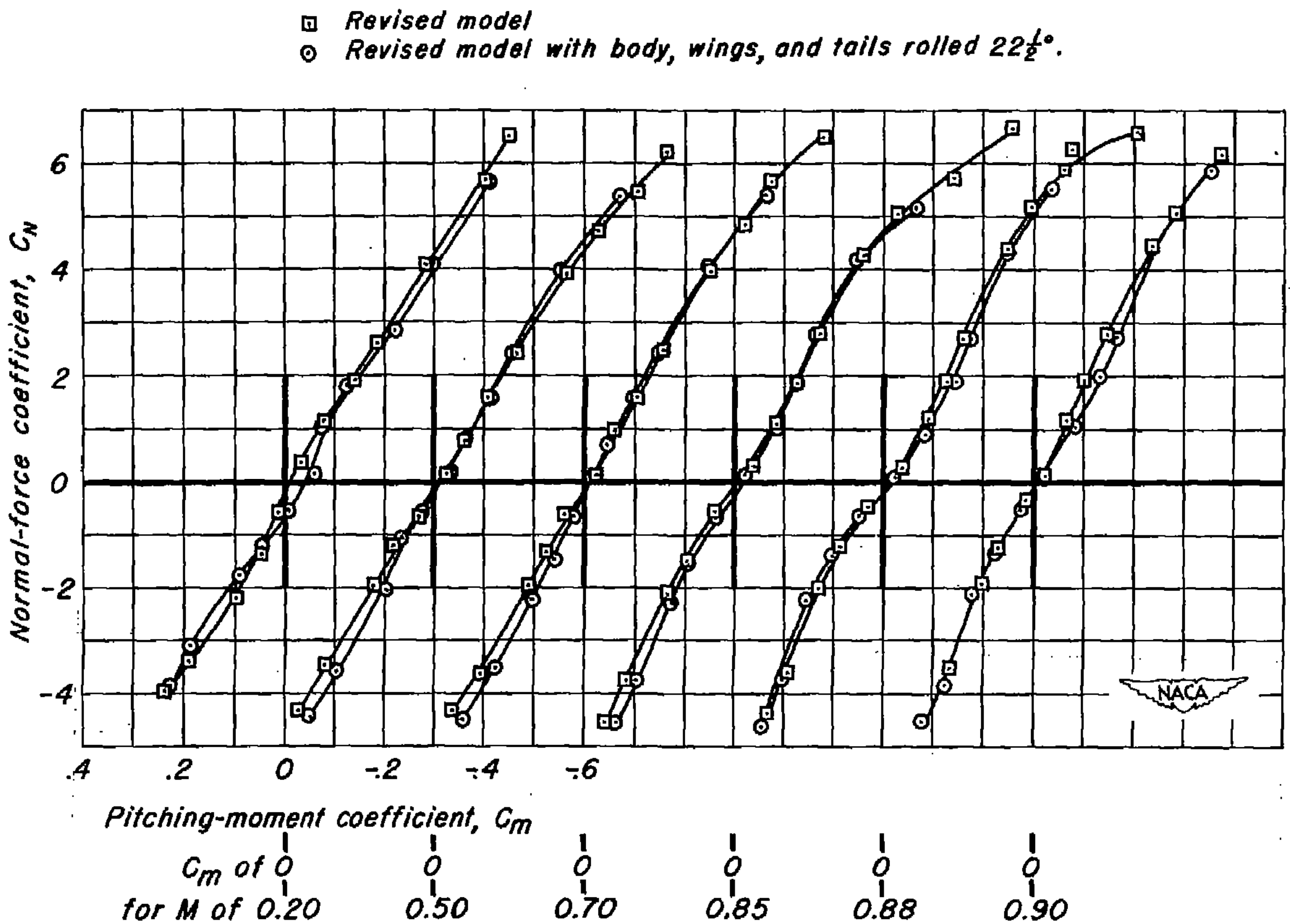

Figure 21.—Variation of normal-force coefficient with pitching-moment coefficient for the revised model with the body, wings, and tails rolled $22\frac{1}{2}°$.

[redacted]

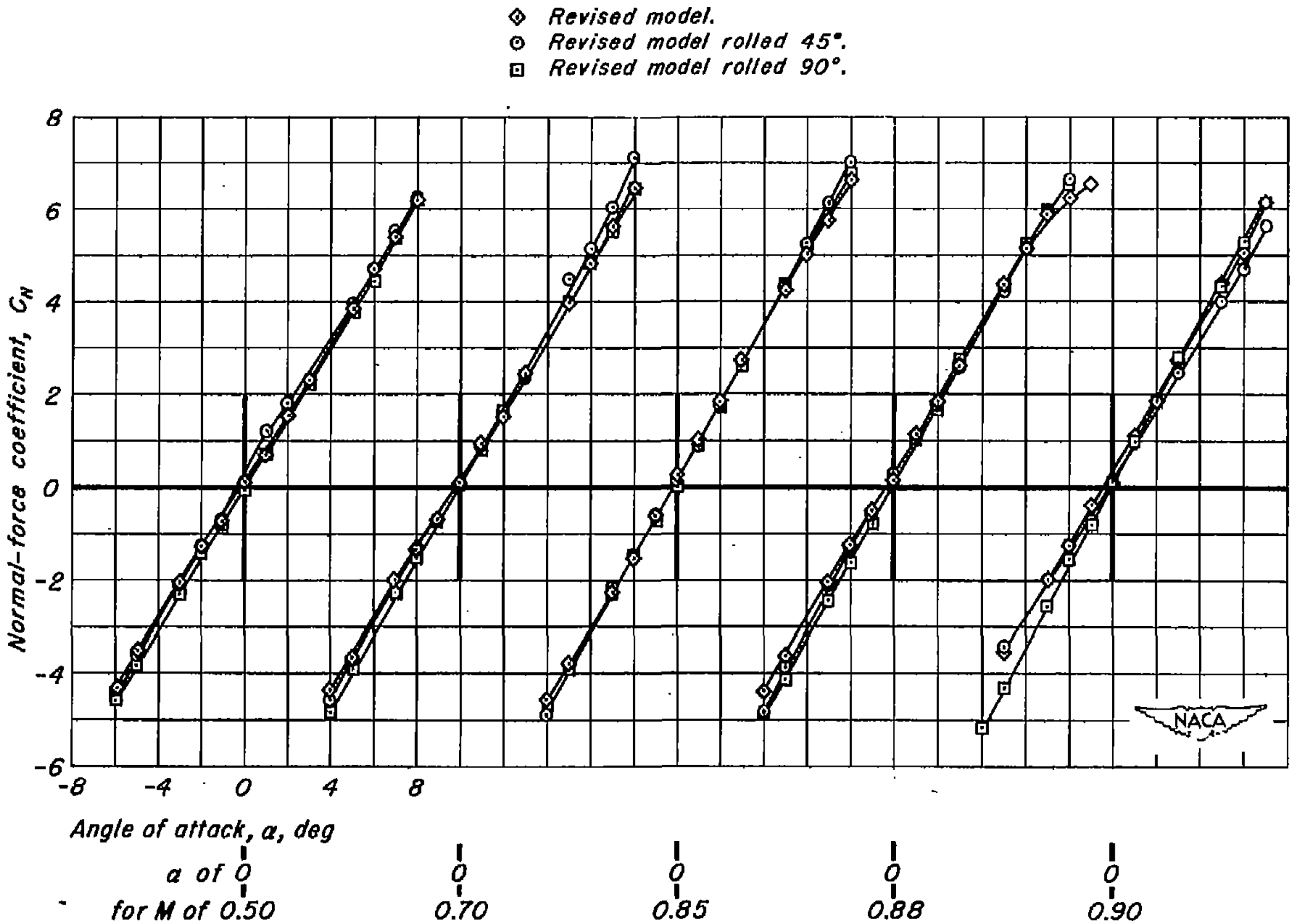

Figure 22.– Variation of normal-force coefficient with angle of attack for the revised model rolled 45° and 90°.

[redacted]

[redacted]

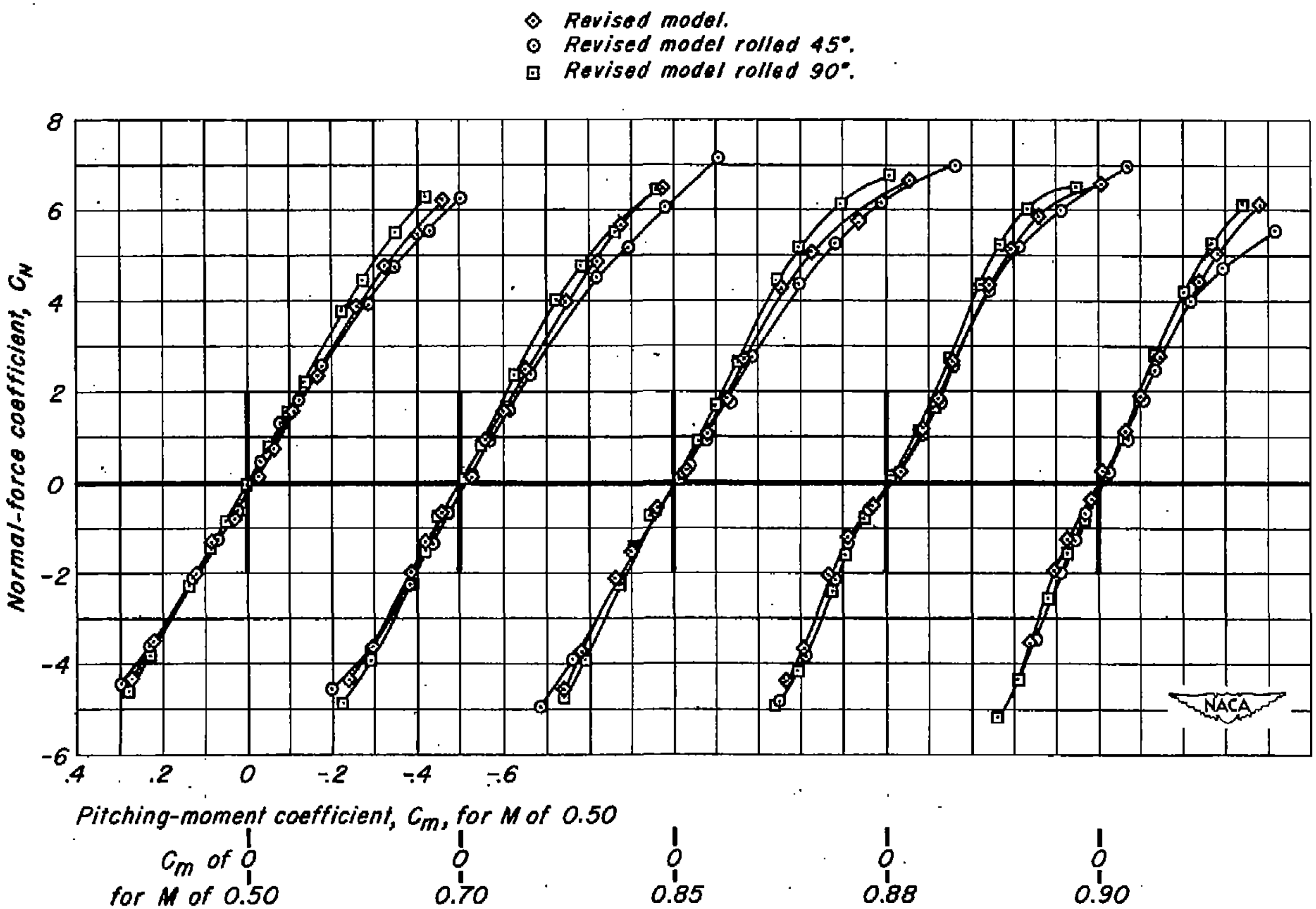

Figure 23.—Variation of normal-force coefficient with pitching-moment coefficient for the revised model rolled 45° and 90°.

[redacted]

[redacted]

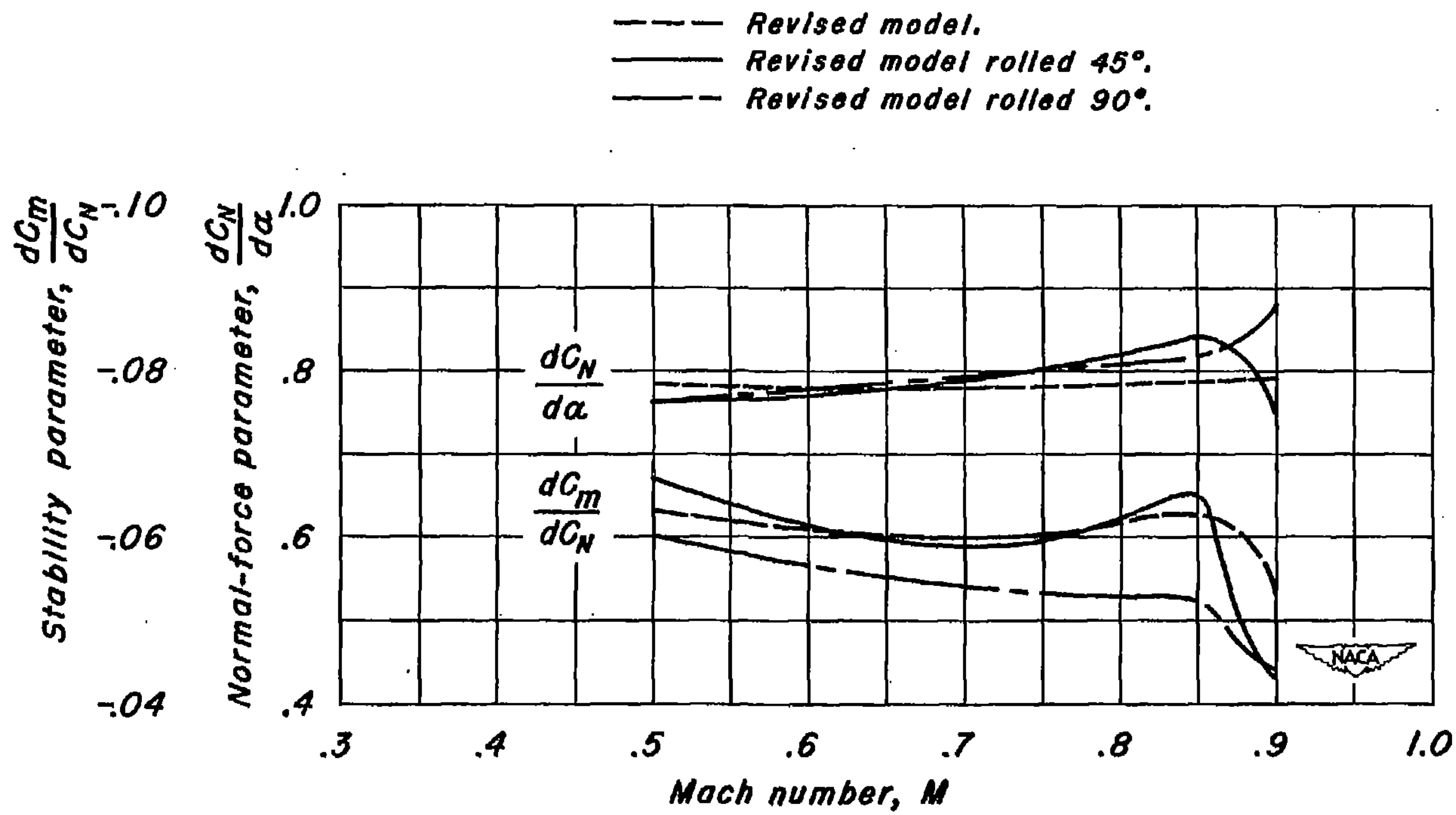

Figure 24.–Variation of normal-force and stability parameters with Mach number for the revised model rolled 45° and 90°.

[redacted]

[redacted]

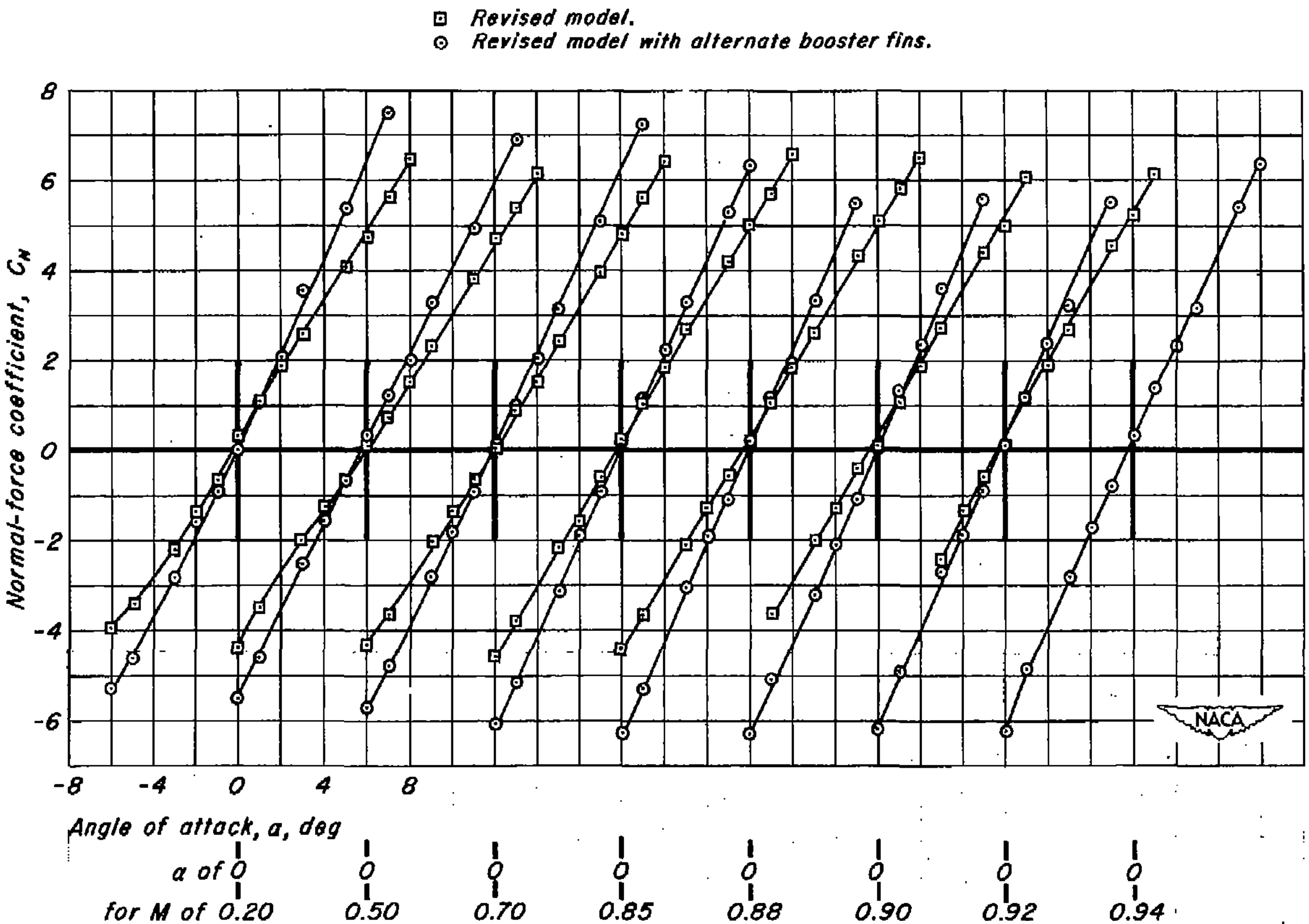

Figure 25.–Variation of normal-force coefficient with angle of attack for the revised model with the alternate booster fins.

[redacted]

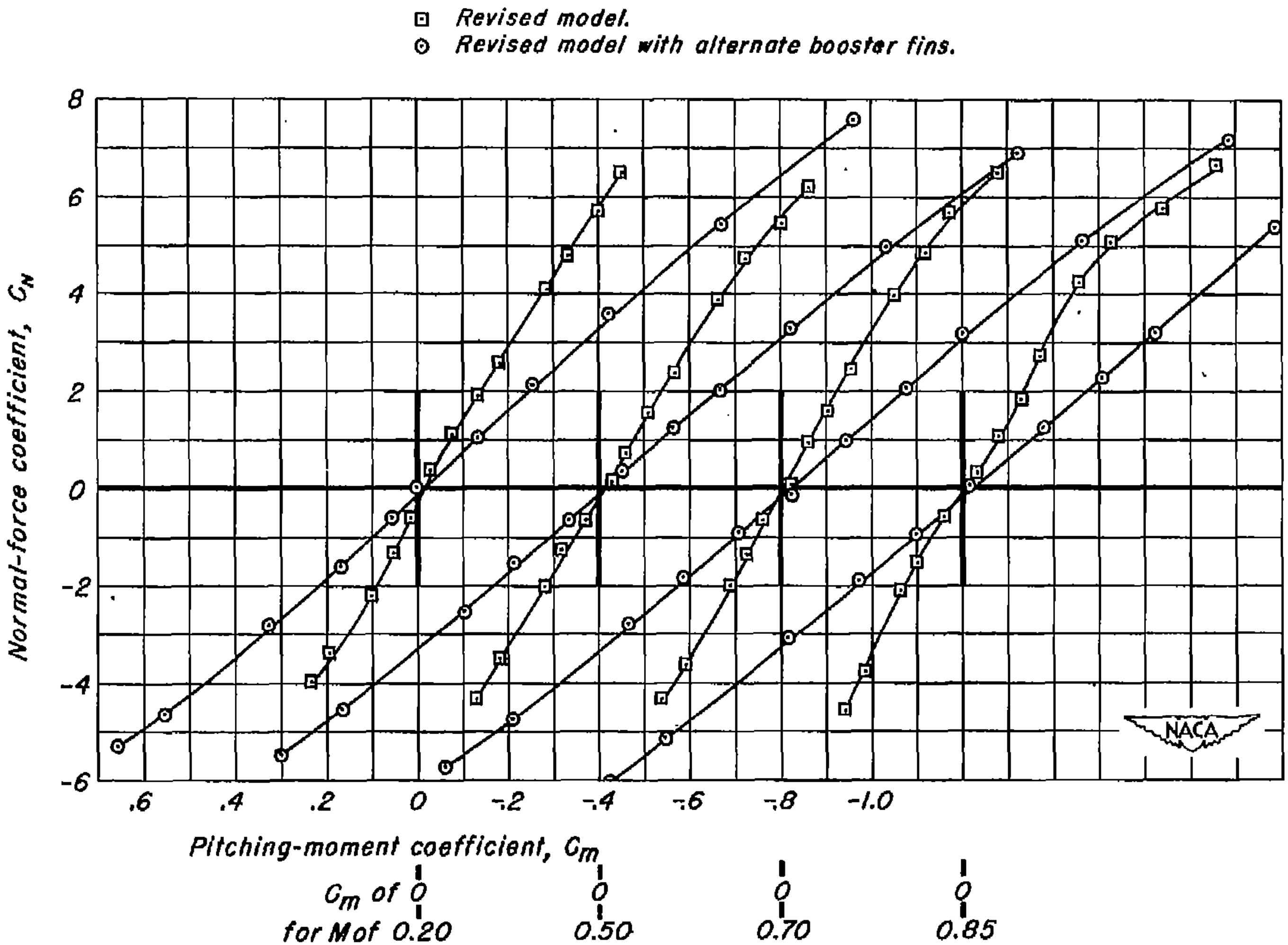

(a) M, 0.20, 0.50, 0.70, 0.85.

Figure 26.–Variation of normal-force coefficient with pitching-moment coefficient for the revised model with the alternate booster fins.

[redacted]

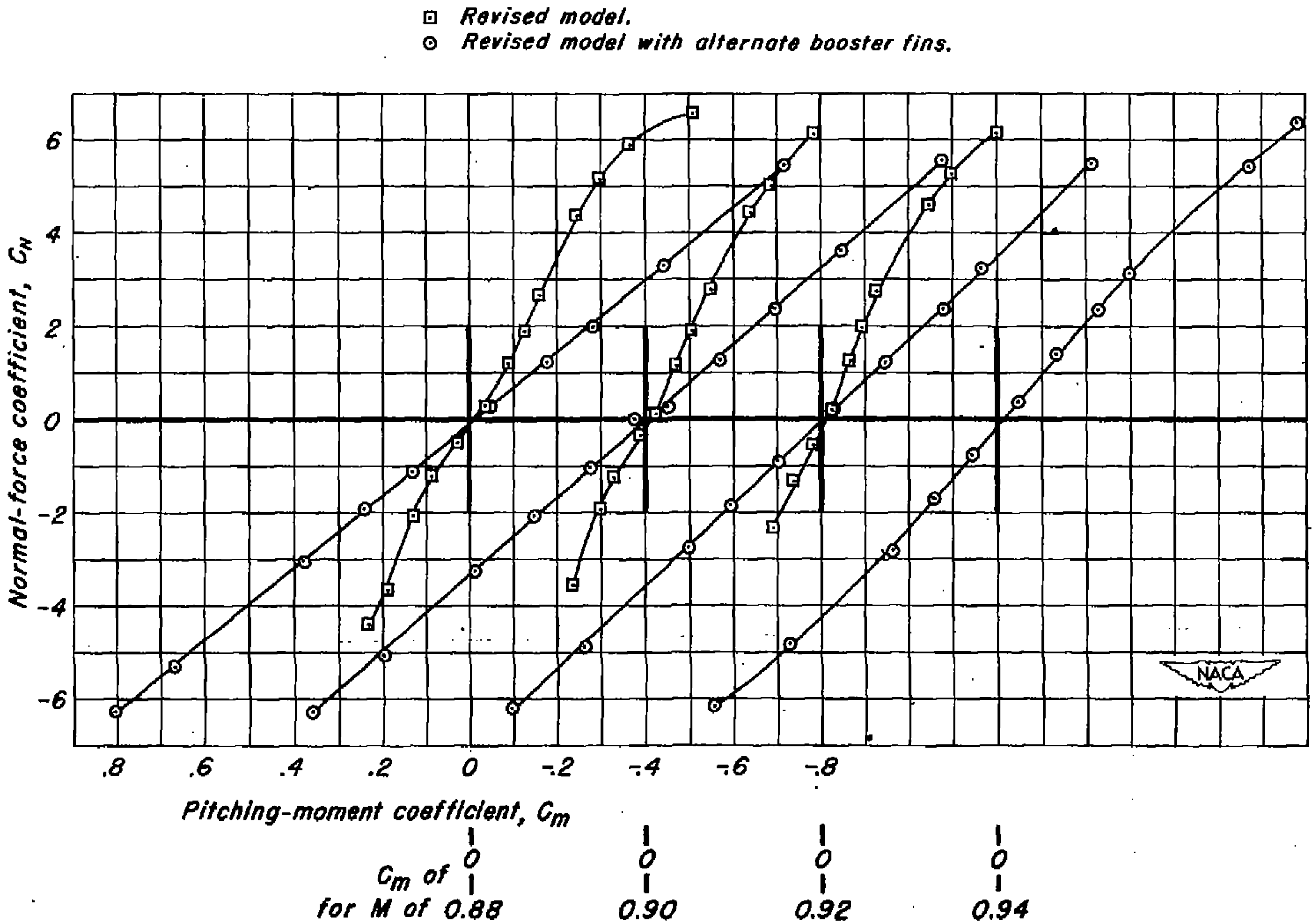

(b) M, 0.88, 0.90, 0.92, 0.94

Figure 26.—Concluded.

[redacted]

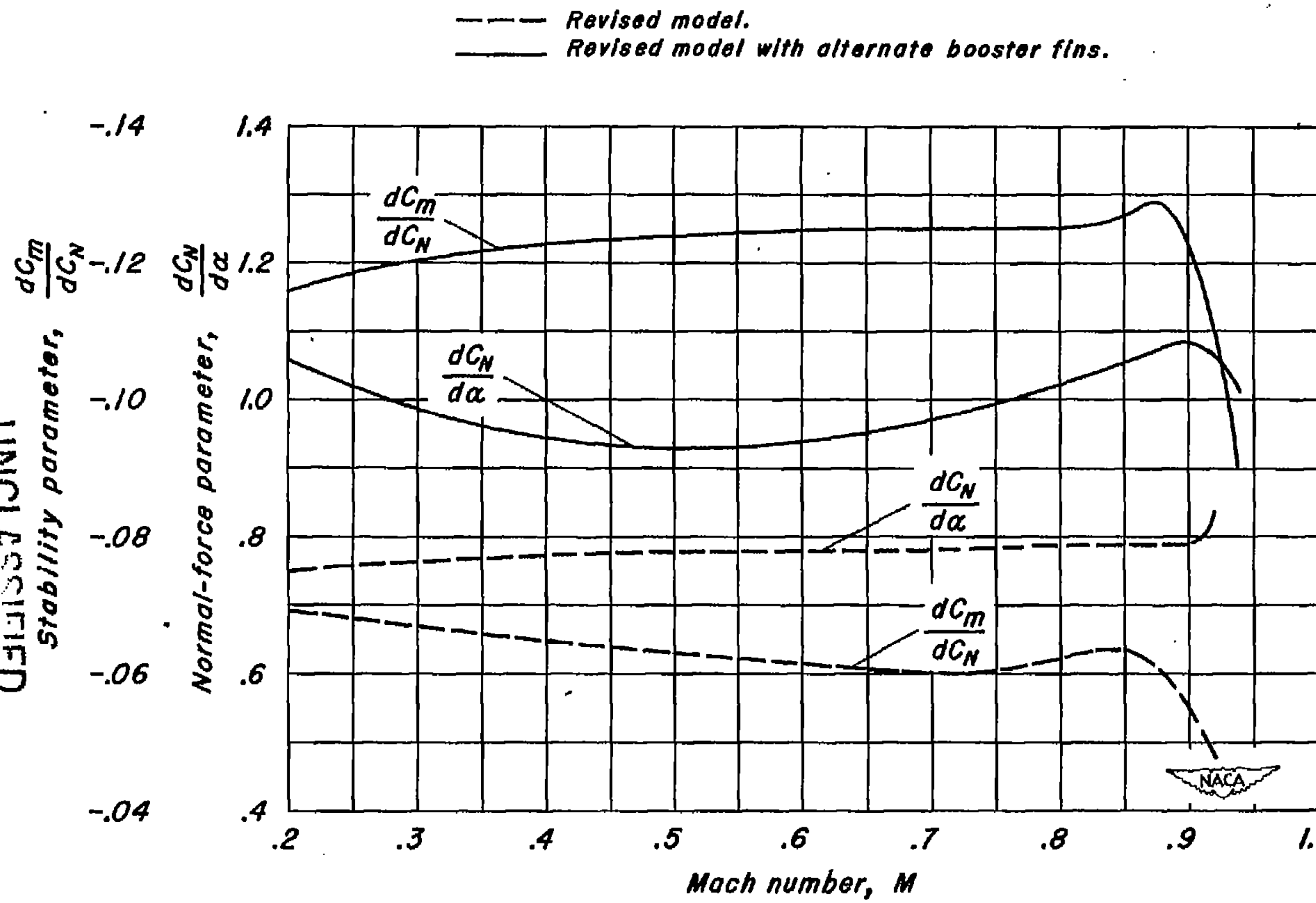

Figure 27.–Variation of normal-force and stability parameters with Mach number for the revised model with the alternate booster fins.